NTNU – Trondheim
Norwegian University of
Science and Technology

DC Grid with Energy Storage for Jack-up rigs

Axel Redse Bratfos

Master of Energy and Environmental Engineering
Submission date: June 2014
Supervisor: Lars Einar Norum, ELKRAFT

Norwegian University of Science and Technology
Department of Electric Power Engineering

Preface

This master thesis concludes my 5-year master's degree in energy and environmental engineering at the Norwegian University of Science and Technology.

I would like thank my supervisor Professor Lars Einar Norum for his encouragement and support through this project. I express my gratitude to Espen Haugan and Sverre Gjerde at Siemens who initiated this project and has helped me along the way. I would also like to thank Eric Cayeux at IRIS for useful inputs on the drilling and mechanical part of this thesis.

Axel Redse Bratfos

Trondheim, June 2014

Abstract

Energy storage systems are used in various applications to compensate for a fluctuating power demand. For a jack-up drilling rig, energy storage can work as a buffer between load motors and diesel generators. During a tripping operation, which involves lifting and lowering of the drill string, the diesel generators limits how fast the motor loads can accelerate. The objective of the work presented in this thesis, was to build a model for simulations of DC grid with energy storage and use this model for a case study to answer how much an energy storage can speed up the operation, and which energy storage technology that is best suited for the purpose.

The studied system was a DC grid for jack-up rigs supplied by diesel generators. Two energy storage technologies were considered; electrolytic capacitors and super-capacitors. The main basis of comparison between these technologies was power- and energy density.

When performing a tripping operation, the load motors have a repeating and fluctuating power demand which changes throughout the operation depending on how heavy the load is. The energy storage will supply the increasing load power while the diesel generators accelerate. It was decided to investigate two scenarios which repeat throughout the tripping process; one for high load, and one for low load.

Several simplifications were made when building a model in Simulink. The model consisted of one diesel generator model, several energy storage modules with DC-DC converters, and a load model. The loads were modelled as a current source which draws a given power based on the measured voltage. The diesel engine was modelled as a first order system, while the generator was modelled using a built in Simulink model. It was found that a two quadrant DC-DC converter was a suitable interface between the energy storage and DC bus. Two energy storage models were developed, one for supercapacitors and one for electrolytic capacitors.

Four simulations were run to compare the two energy storage technologies and to investigate the two different load scenarios. The results indicated that an energy storage can reduce the time duration of a tripping operation with 11-16%. It was also found that the supercapacitors had the best power- and energy density for the studied load scenarios. Over all, the model worked properly and gave trustworthy results.

Sammendrag

Energilager blir brukt til ulike formål, for å kompensere for et varierende effektbehov. For en Jack-up borerigg, kan et energilager fungere som en buffer mellom lastmotorer og dieselgeneratorer. Under en tripping operasjon, som innebærer løfting og senkning av borestrengen, utgjør dieselgeneratorene en begrensning for hvor fort lastmotorene kan akselerere. Målet med denne avhandlingen, var å bygge en modell for simulering av DC-nett med energilager, og bruke denne modellen for å gjennomføre et case-studie som kan svare på hvor mye et energilager kan effektivisere operasjonen tidsmessig, samt å avgjøre hvilken energilagringsteknologi som er best egnet for dette formålet.

Det studerte systemet var et DC-nett for Jack-up rigger forsynt av dieselgeneratorer. To energilagringsteknologier ble vurdert; elektrolytiske kondensatorer og superkondensatorer. Det viktigste sammenligningsgrunnlaget mellom disse teknologiene var effekt- og energi-tetthet.

Under en tripping operasjon utgjør lastmotorene et repeterende og varierende effektbehov som endres gjennom hele operasjon avhengig av hvor tung lasten er. Energilageret må forsyne den gitte laststrømmen mens dieselgeneratoren akselereres. Det ble besluttet å undersøke to scenarier som gjentas gjennom hele tripping prosessen; en for høy last, og en for lav last.

For å lage en modell i Simulink måtte problemstillingen og systemet forenkles. Modellen bestod av en diesel-generatormodell, flere energilagermoduler med DC-DC-omformere, og en lastmodell. Lasten ble modellert som en strømkilde som trekker en gitt strøm basert på den målte spenning. Dieselmotoren ble modellert som et første ordens system, mens generatoren ble modellert ved hjelp av en innebygd Simulink modell. En to-kvadrants DC-DC-omformer viste seg å være tilstrekkelig, som grensesnitt mellom energilageret og DC-bussen. To energilagermodeller ble utviklet, en for superkondensatorer og en for elektrolytt-kondensatorer.

Fire simuleringer ble kjørt for å sammenligne de to energilagerteknologiene og å undersøke de to lastscenariene. Resultatene indikerte at et energilager kan redusere varigheten av en tripping operasjon med 11-16%. Det ble også konkludert med at superkondensatorer hadde den beste effekt- og energitettheten for de studerte lastscenariene. Modellen viste seg å fungere godt og ga troverdige resultater.

Acronyms

In this paper the following acronyms are used:

ES=Energy Storage

DC = Direct current

AC = Alternating Current

HV = High voltage

LV = Low Voltage

SiC = Silicon Carbide

IGBT = Insulated gate bipolar transistor

PWM = Pulse width modulation

ESR = Equivalent series resistance

EPR = Equivalent parallel resistance

Eq = Equation

UPS = Uninterruptable power supply

PI = Proportional Integral controller

EDLC = Electric double-layer capacitors

Ref = Reference

pu = per unit

VC = Voltage Control

CC = Current Control

RMS = Root mean square

Contents

1 Introduction

1.1 Background and Problem description

Recent research has resulted in wide use of energy storages (ES) for several applications such as electrical vehicles, diesel electric ships, or in relation with renewable energy production. There has also been an increasing attention around energy use in the oil and gas industry. Offshore drilling rigs are mobile units that perform exploration to develop new oil or gas fields. Drilling operations require heavy power consuming electrical motors which represent the main load on the vessels grid. The isolated grid of the drilling rig is usually supplied with diesel generators, in contrast to production platforms which can be powered by gas turbines or HVDC transmission from land. Introducing an energy storage such as a capacitor bank may allow the motor loads to be operated more efficiently and may result in lower fuel consumption and emissions.

The first objective of this project is to study how an energy storage system can improve efficiency of drilling operations for offshore drilling rigs and decide which requirements this sets for the energy storage. The specific power system studied is a DC-grid for jack-up rigs. The ES is intended to improve efficiency of a tripping operation, which involves lifting and lowering of the drill string and causes large variations in electrical load. An ES can smooth out load fluctuations on the diesel generators, allowing the motor loads to operate more independent from the diesel generators to speed up the tripping operation.

The studied load scenarios require an ES technology that can deliver rapidly increasing currents and high power. The second objective of this thesis is to investigate which ES technology is best suited for the studied load scenario. Mainly two technologies are considered; electrolytic capacitors and supercapacitors. Comparing these technologies involves evaluating efficiency, energy- and power density.

To solve the problem, the system is modelled in Simulink. The model itself is an important product of this project and can be used for further studies of Energy Storage and DC-grids. Building a model of the system requires study of the load situation, energy storage technologies, DC-DC converters and marine DC-systems with diesel generators.

1.2 Problem limitations

Although energy storage may be relevant to other types of drilling rigs or ships, this study is limited to only considering one load situation. The goal is to investigate how energy storage can speed up the process, other side effects such as improved fuel economy or reduced emissions are not studied in detail. As mentioned only two ES technologies are considered and they are both considered separately, not as part of a hybrid ES system. Only LV systems are considered, and the model is based on capacitor modules with 450-500V nominal voltage. Several topics and challenges related to ES are not studied in detail, such as faults, stability, safety and thermal aspects. Modelling the system involves simplifications to reduce simulation time and the complexity of the problem.

2 Theory and System Description

2.1 Jack-up rigs

Jack-up rigs are the most popular type of offshore drilling units for offshore exploration and development purposes [1]. In contrast to semisubmersible rigs or drill ships, the jack-up is self-elevating and rest on the sea floor [1]. Jack-up rigs are still considered mobile offshore drilling rigs, although most of them do not have their own propulsion system and rely on outside sources for movement [1]. They are most suitable for shallow waters, typically less than 100m [1] [2]. Figure 2.1 shows a typical Jack-up Rig in the North Sea with three legs. The Derrick, a tall frame work structure mounted on the side of the platform, contains a rope and pulley system for raising and lowering heavy equipment, mainly the drill string.

Figure 2.1 - Jack-up rig in the North Sea

2.2 DC grid for Jack-up rigs

DC power systems are considered advantageous for low and medium level power systems due to the fact that power electronic loads often needs DC power for end use or DC interfaces [3]. Although most drilling rigs today have an AC system, using LVDC systems is an increasing trend, especially for ships with diesel-electric propulsion, and is expected to give several benefits regarding space utilization, weight, fuel consumption and emissions [4].

Power grids for jack-up rigs have much in common with systems for drilling ships, production platforms and other marine grids. For safety reasons, the system is divided into several autonomous parts, often 2-4 switch boards with an equal number of generators and loads. Figure 2.2 displays a One-line diagram for a DC system with two switchboards. The two 930V busses are connected with an IGBT bridge, which is closed during normal operation allowing load sharing between all the generators.

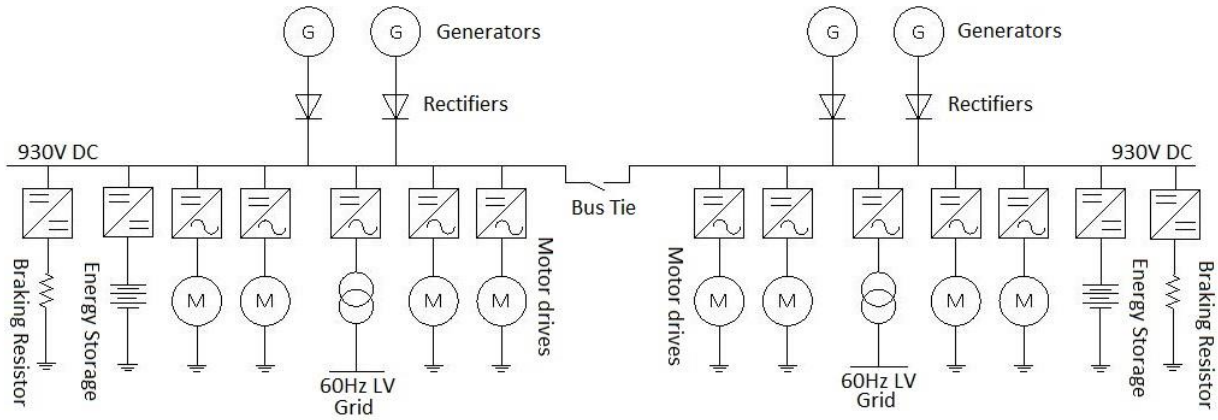

Figure 2.2 - Oneline diagram, Jack-up rig with Energy Storage

2.2.1 Diesel Engine, Generator and Rectifier

As for most drilling rigs, the system in Figure 2.2 is powered by diesel engines. For an AC system, the speed of the diesel engines is bound by the electrical frequency of the system. But with DC, the diesels can run at optimal speed for the given load power, in terms of fuel economy or efficiency. The fact that switchboards are connected during normal operations offers even more flexibility, for instance for low loads where one generator can power the whole system. Smart operation of the diesel/generators can thus result in lower fuel costs and less CO2 and NOx emissions. But there are also other factors inflicting the operation of the diesels. For safety reasons, the generators must be able to handle sudden load increases, which may involve idle running of the generators. Here an ES could work as a buffer, giving the diesel engines time to accelerate. A diesel engine typically needs 10-20 seconds (Appendix 1) from zero to full speed.

When studying the system from an electrical/power perspective, diesel engines are often modelled as a first order system. In other words, the diesel engine is seen only as a delay in changing rotational speed or torque, where the generator model can either take torque or speed as an input. In contrast to an AC system, reactive effect control is not necessary. Instead, the excitation system will regulate the output DC voltage from the rectifier.

The studied system has 3333VA 690V wound rotor generators in series with 6 puls diode rectifiers. The resulting bus voltage, V_{DC} is 930V, calculated using Eq. 2.1 for a full-bridge three-phase diode rectifier [5], where V_{LL} is the line to line voltage of 690 V_{rms} on the AC side.

$$V_{DC} = \frac{3\pi}{\sqrt{2}} V_{LL} \qquad \text{Eq. 2.1}$$

The output voltage from a 6 puls rectifier usually results in considerable output ripple which require filters on the DC bus. The need for big capacitor banks are often considered one of the draw-backs with having a DC system.

2.2.2 Loads

As displayed in Figure 2.2, most of the loads in the system are variable speed motor drives. There are also transformers supplying a low voltage grid with various smaller applications. But the main loads are the variable speed controlled induction motors that run the drilling equipment. The most power consuming loads are the topdrive, which provides the circular torque of the drill string and drill bit, mudpumps, which circulate the drilling fluid, and draw-works, which is machinery used to hoist and lower the drill string. Some jack-ups also have thrusters for propulsion or station keeping.

In this project, the main focus will be on the draw-work, which is further described in section 2.5. The draw work can also deliver breaking energy back to the system which is handled by breaking resistors or energy storage.

2.3 Energy Storage Technologies

2.3.1 Motivations

Energy storage systems are used for numerous applications; in ships, electrical vehicles, and grid applications [6] [4] [7] [8] [9]. On drilling rigs, an ES can decouple the energy generation from the demand to smooth out the load on the generators or address power quality issues [10] [11]. ESs may also serve as emergency/back-up power similar to uninterruptable power supplies (UPSs). The motivation for including an ES system is decisive for which technology to use. There are many technologies available for converting and storing electrical energy, all with different properties in form of power density, energy density, efficiency, life time, reliability, maintenance, grid interface and costs.

2.3.2 Batteries

Battery technology has improved the last decade as a result of extensive research. Lithium ion batteries have replaced many of the older types of batteries such as NiCD, due to its high energy-to-weight ratio and low self-discharge [10]. Li-ion batteries can also operate with high current levels compared to other batteries, but they do have considerable internal resistance which implies a risk for heat-up and failure [10]. Due to the development with li-ion technology, batteries are often considered a natural choice for energy storage systems. The terminal voltage keeps fairly stable when the batteries are over 20% charged, so they do not necessarily need a converter and can be connected directly to the DC bus. But the fact that a battery can only handle small variations in voltage, may limit the flexibility of the system. For the studied problem where the ES is supposed to work as a buffer to allow fast load increases, batteries will not endure the rapidly fluctuating power demand. A combination of battery and capacitor on the other hand could prove to be a good choice, but batteries are outside the problem definition of this thesis.

2.3.3 Capacitors

As opposed to other energy storage technologies such as batteries flywheels or super conducting magnets, capacitors have the ability to store electric energy directly without converting it [12]. Inherently they feature almost endless cycle lives, minimal loss, good Coulomb efficiencies and quick recharge [12]. Capacitor energy storage is therefore a natural choice to compensate for fluctuating power [13].

$$E = \frac{1}{2}C \times ({V_1}^2 - {V_2}^2) \qquad \text{Eq. 2.2}$$

Energy stored in a capacitor is given by Eq. 2.2 from [7]. C is the capacitance measured in Farad, V_1 is the rated voltage and V_2 is the voltage after discharge. From an energy perspective, choosing a low discharge voltage is a space- and weight saving way to increase energy capacity. At the same time one wants the energy storage to be able to supply a certain power. A low discharge voltage means that the capacitor will need to supply higher currents to supply constant power.

2.3.4 Electrolytic Capacitors

Electrolytic capacitors are associated with high capacitance values, low costs and medium frequency levels. Among these, aluminium electrolytic capacitors have been considered the first choice for high voltage ES due to high capacitance per volume and handling high voltages [7].

An electrolytic capacitor ES will consist of multiple capacitors to achieve high enough energy capacity. Connecting capacitors in parallel means that the total capacitance of the ES is a sum of the capacitance of the individual capacitors. While the total internal resistance of the ES is decreasingly proportional to number of capacitors. Parallel connection of the capacitors also increases the rated maximum current- and thereby power capacity of the ES.

2.3.5 Supercapacitor

Supercapacitors, also known as ultracapacitors or electric double-layer capacitors (EDLC), work in much of the same way as conventional capacitors, but with much higher energy density [10]. They are safer and have longer service life than batteries and require virtually no maintenance [13]. A disadvantage with Supercapacitors is that each individual cell has a dielectric voltage withstand of 3V or lower [13]. Higher voltage capacitor banks will therefore require several cells in series, resulting in high internal resistance. Heating is also a concern with Supercapacitors. Since losses, and hereby heat generation, are directly proportional to squared current [13], thermal issues set the limits for how much current the Supercapacitor can handle over time.

Super Capacitors are a promising technology for energy storages, especially in combination with for example batteries. They are considered most relevant for short time-duration applications with pulses lasting less than 40 seconds [8].

2.3.6 Comparison

The electrolytic- and Supercapacitors share many advantages compared to other ES technologies. Table 2.1 shows typical values for the different technologies, based on ref [14] and [10]. Figure 2.3 shows power- vs energy density for the different technologies based on data from ref [14] and [10].

Technology	Energy efficiency [%]	Energy Density [Wh/kg]	Power Density [W/kg]	Cycle life [# cycles]	Self-Discharge
Lithium-ion	70-85	100-200	360	500-2000	Medium
Supercapacitors	95	<50	4000	>50000	High
Electrolytic Capacitor	99	0.01-0.07	3000-10^7	0.6-12million	Very High

Table 2.1 - Comparison of ES technologies, typical values

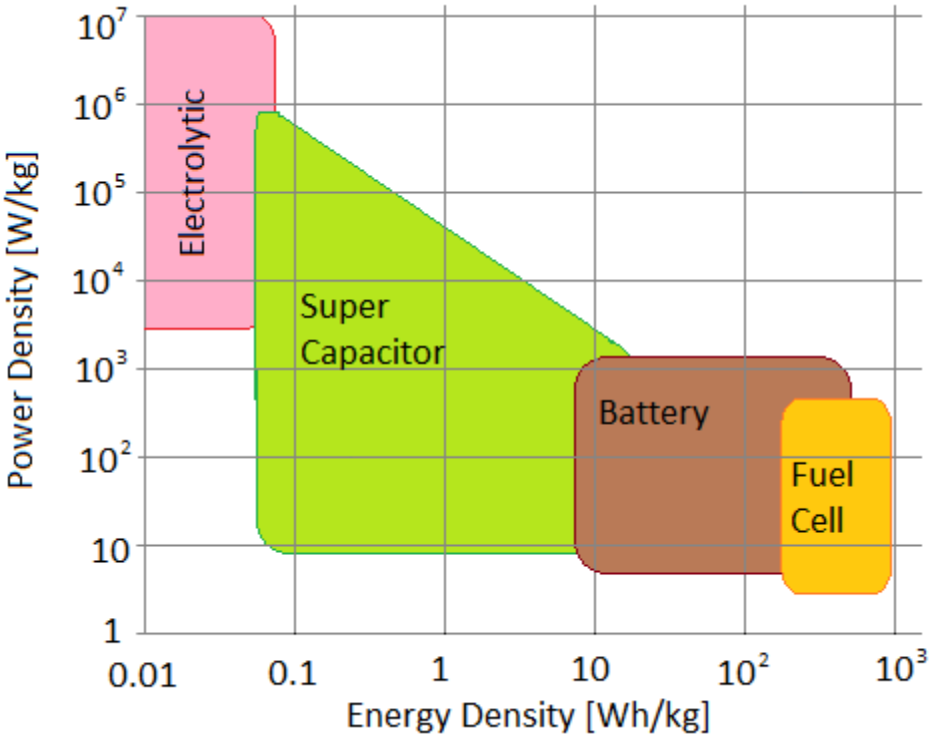

Figure 2.3 - Power- and Energy Density for different ES technologies

2.3.7 Modelling Capacitor ES

Any electrolytic- or Supercapacitor has some inductances and distributed resistances [15]. A typical equivalent circuit for capacitors is shown in Figure 2.4 [16] [17]. The equivalent parallel resistance (EPR) represents a leakage current effect which has a long-term effect on the performance of the ES [16], but can be neglected in short-term models. The equivalent series resistance (ESR) for electrolytic capacitors is smaller than for Supercapacitors, but is usually included in models [7]. Alternatively a capacitor ES could be modelled with

distributed parameters to better simulate the thermal behaviour of the capacitor more accurately [13].

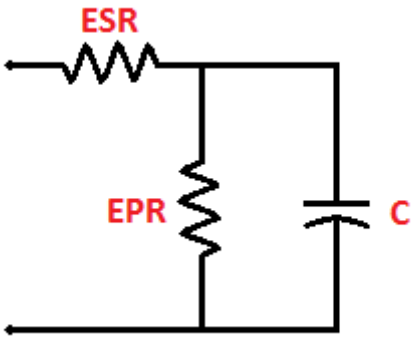

Figure 2.4 - Capacitor equivalent circuit

2.4 DC-DC converter for Energy Storage

2.4.1 Requirements

DC-DC converters are a necessity in capacitor energy storage systems due to the fact that the ES voltage varies considerably as the capacitor discharges. A bidirectional DC-DC converter will form the interface between the energy storage and bus and has mainly two purposes; compensating for the voltage difference between the ES and the bus, and controlling the power flow to discharge or recharge the ES. Based on ref [7]'s requirements for a HVES for grid applications and the system described in section 2.2, a converter for capacitor ES should be able to:

- Use the bus voltage to charge the ES.
- Quickly maintain and regulate the bus voltage during a load increase or power interruptions on the bus.
- Minimize power consumption when the ES is not charging or discharging.
- Minimize the size of the capacitor bank.
- Automatically discharge the capacitors during shutdown of the system.
- Handle inrush currents during initial recharge and handle short-circuit currents.
- Minimize EMI requirements, thermal limitations, weight, volume and costs

For the studied system however, the most important factors will be charging and discharging of the ES under normal (steady state) conditions.

2.4.2 Buck/Boost converter

When choosing a power bridge configuration for the converter, one must firstly consider current direction and voltage polarity. An ES system will always require bidirectional current flow, but whether the voltage is higher on the ES or the Bus side of the converter depends on the design of the energy storage. In a system where the ES voltage is always lower than

the bus voltage, a two-quadrant converter, such as the buck/boost converter will be sufficient.

The buck/boost power bridge, illustrated in Figure 2.6 is a simple configuration requiring only two switches (IGBTs) [7], and allows 2-quadrant operation (Figure 2.5). This project is limited to study a LVDC system where the ES voltage is much lower than the main switchboard.

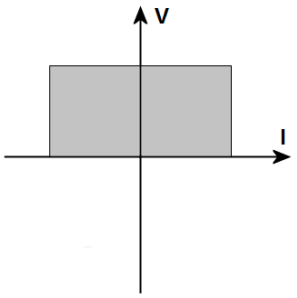

Figure 2.5 - 2-quadrant operation

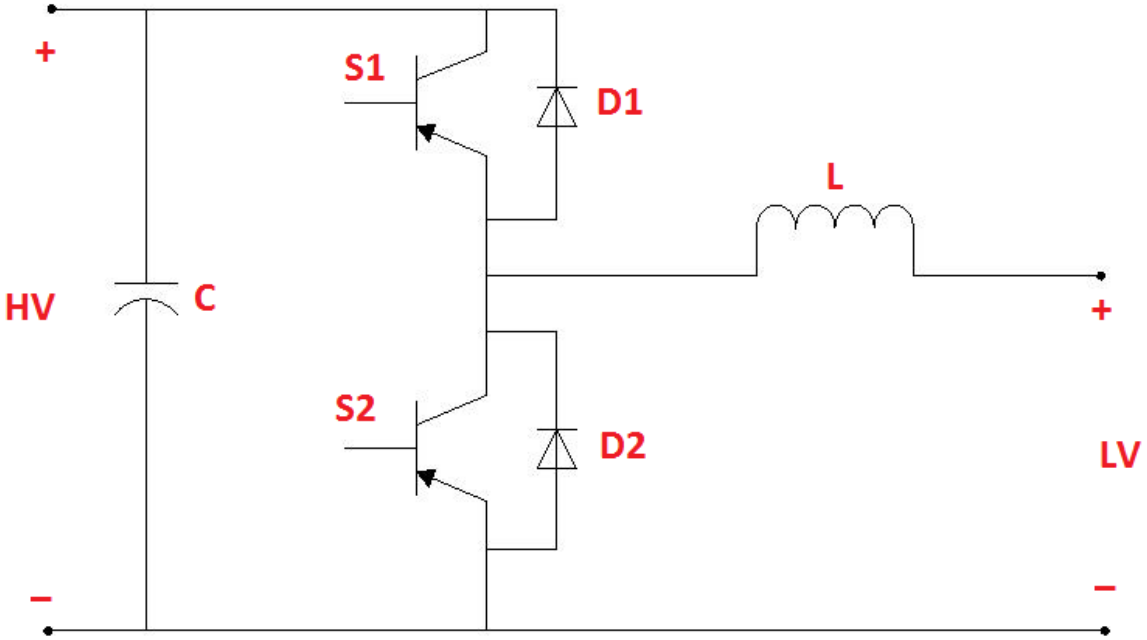

Figure 2.6 - Buck/Boost converter

With the ES on the LV side and DC bus on the HV side, the converter will operate as a buck converter when charging the ES, and boost converter during discharge, as described in Figure 2.7. Voltage gain for buck and boost operation with continuous conduction mode is given in Eq. 2.3 and Eq. 2.4 respectively, where D is the duty cycle and η is the efficiency of the converter.

$$\frac{V_{LV}}{V_{HV}} = D\eta \qquad \text{Eq. 2.3}$$

$$\frac{V_{HV}}{V_{LV}} = \eta \frac{1}{1-D} \qquad \text{Eq. 2.4}$$

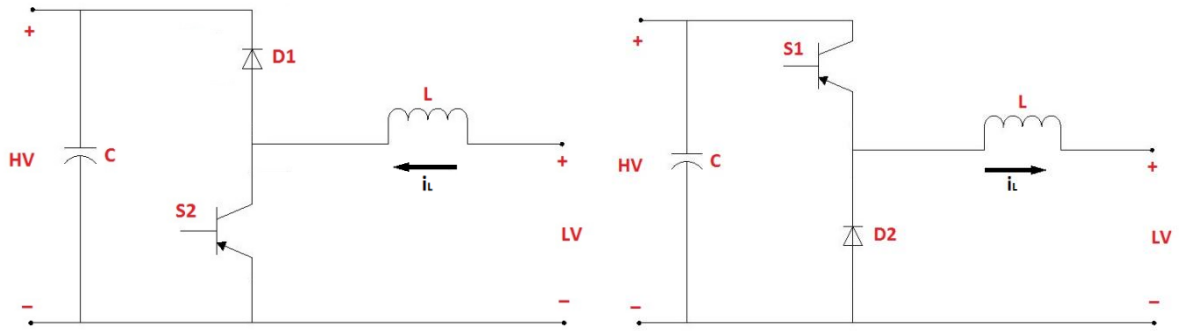

Figure 2.7 - Converter in boost mode (left) and buck mode (right)

2.4.3 Converter operation

Operation and control of the ES should be designed on the basis of known load scenarios, ensuring that the ES has available energy in case of load increases. The bus voltage represents a common reference for both loads and generators. If the generators are not able to deliver the required load, the bus voltage will start decreasing. When the bus voltage reaches a certain level, loads will be disconnected to reduce the power demand. The energy storage should detect and compensate for the voltage decrease before the loads have to cut power. Figure 2.8 illustrates how the energy storage has three operational modes based on the bus voltage. Due to leakage currents in the capacitors, the ES will require some power to maintain full voltage, hence representing a constant loss when it is not in operation.

From an energy saving perspective, the ES should also have available capacity to receive power, in case of voltage decrease on the bus. Breaking power from the load motors are usually handled by breaking resistors. This energy can alternatively be stored in the ES, which will make the rig more energy- and fuel efficient.

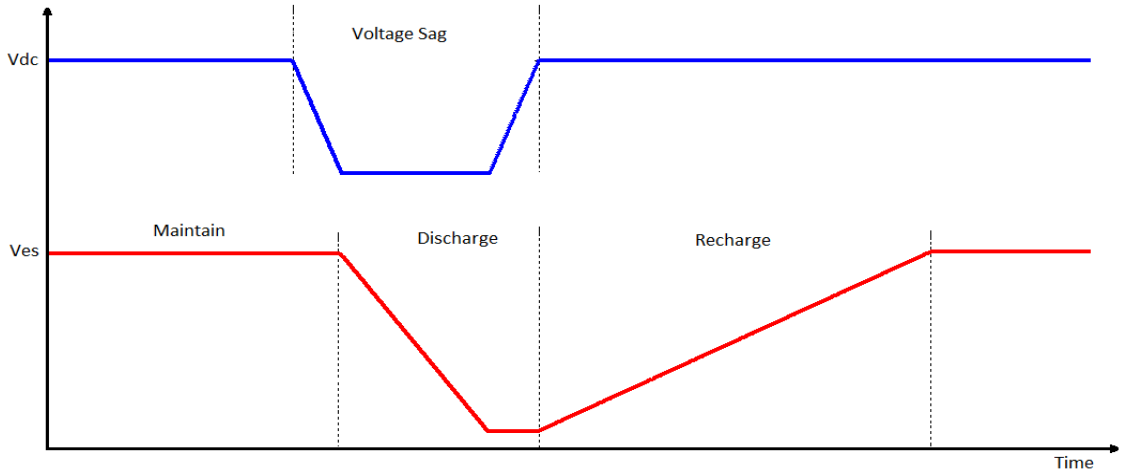

Figure 2.8 - ES and Bus voltage during voltage sag

2.4.4 Dimensioning converter components

When designing the converter, the discharge mode of the converter should be considered first, as this mode demands high power and fast response time [7]. As discussed, the converter is operating in boost mode during discharge, so the converter can be designed as if it were a boost converter [7].

The inductor will have to carry the full load current added to the ripple current [7]. Neglecting diode voltage drops, maximum peak inductor current can be estimated using Eq. 2.5.

$$I_{L,max} = \frac{P_{ES}}{V_{ES}} + \frac{1}{2} \times \Delta I_L \qquad \text{Eq. 2.5}$$

The inductor ripple, ΔI_L, will not be constant during operation, as it depends on the ES voltage. Eq. 2.6 shows how minimum inductor size can be calculated for boost converters, assuming continuous conduction mode and lossless converter [18]. This equation can be used to approximate minimum inductor size for a known frequency and acceptable current ripple.

$$L_{min} = \frac{V_{LV}(V_{HV} - V_{LV})}{f_s \cdot \Delta I_L \cdot V_{HV}} \qquad \text{Eq. 2.6}$$

The inductor size has a strong influence on transient response [7]. Choosing a low inductance will theoretically allow higher di/dt and faster response [7], a small inductor will also reduce the physical size and weight of the converter. A large inductance will allow the converter to stay in continuous conduction mode at lower load levels, and reduce current ripple. Alternatively the single coil could be replaced by a high frequency transformer which would offer a galvanic division of the ES and the rest of the system.

Selecting switches and diodes for a converter is a trade-off between size and efficiency. With voltages around 1000V, IGBTs is a valid choice [5]. Switching frequencies for these kinds of converters is typically 2500-5000 Hz, well within the limits for IGBTs which can handle a switching frequency of up to 100 kHz [5]. Choosing a high switching frequency will give higher switching losses but will reduce ripple current.

The bus side capacitor filters the high-frequency current ripple to ensure a stable voltage output. Eq. 2.7 from [18], can be used to adjust the capacitance for a desired voltage ripple. Capacitors with low internal resistance are often preferred, as the resistance adds additional voltage ripple. This ripple is given in Eq. 2.8 from [18].

$$C_{min} = \frac{I_{out,max} D}{f_s \Delta V} \quad \text{Eq. 2.7}$$

$$\Delta V_{ESR,ripple} = R_C * \left(\frac{I_{out,max}}{1 - D} + \frac{\Delta I_L}{2} \right) \quad \text{Eq. 2.8}$$

2.4.5 Converter efficiency

Modelling the converter involves simplifications to reduce simulation time and avoid unnecessary calculations. This can be achieved by using ideal components, neglecting some of the losses in the converter. Power losses in the converter are strongly dependent on the magnitude of the current, and they increase as the voltage on the ES side droops [19]. The losses mainly consists of snubber losses, switching losses, conduction losses in the IGBT, copper losses and core losses in the inductor. Due to advances in power device technology the last decades, bidirectional DC-DC converters can operate at an efficiency of 97% [19]. When SiC power devices become more available, efficiencies as high as 99% is expected [19]. The efficiency of the converter will affect the design of the energy storage itself, as converter losses has to be compensated by bigger energy capacity in the ES.

2.5 Load Scenarios

2.5.1 Tripping

A tripping operation involves raising or lowering the whole drill string which may stretch hundreds of feet from the platform deck to the bottom of the well. It is usually performed to change the drill bit or other parts of the drill string. Tripping may take several hours and represent a stop in the drilling process, which is expensive for the operator who is renting the rig on a daily lease. The typical electrical load during tripping contains repeating variations which can be challenging for the diesel engines. Energy Storage may be used to reduce stress on the diesel generators and reduce the duration of a tripping process.

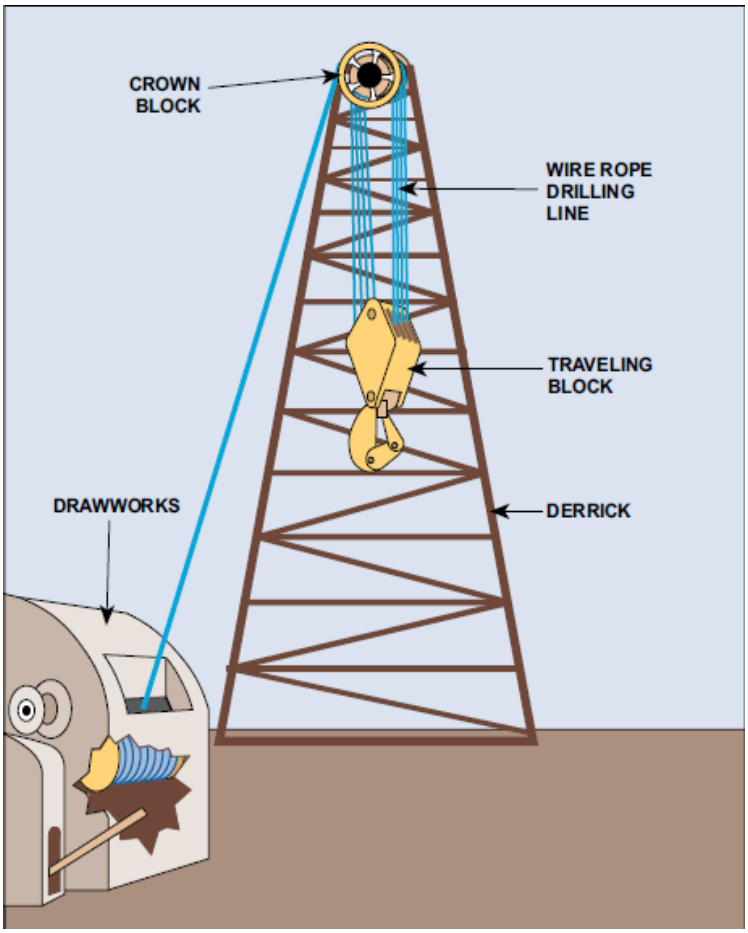

Figure 2.9 - Drawworks and Derrick [32]

The drill string is lowered or hoisted using a system with a winch, called the draw-works, as seen in Figure 2.9. During tripping the draw work motors represent the main load on the grid, as most of the motors associated with drilling (such as top drives) are not in use. On modern drilling rigs, tripping is an automated process. The drill string consists of several segments of equal length (usually 30m). Raising the whole drill string is a repeating process where one segment is lifted at the time, disconnected from the hook, stacked, and the hook is lowered and connected to the next segment of the drill string. When the drill string is lowered, each segment is connected, lowered, then disconnected from the hook and the hook is hoisted back up. These repeating load patterns involve rapid changes in power demand as the draw-work motors is accelerated to lift and decelerated to lower the drill string.

If an ES is going to improve efficiency during tripping, one premise is that the diesel engines/generators are the limiting factor of how fast the process can be executed. This may not always be the case. During tripping in open-hole (close to the reservoir), a major limitation is the generation of downhole pressure pulses, swag and surge [20]. These can cause serious incidents like formation fluid influx, formation collapse or formation fracturing.

Acceleration/deceleration of the drill string is very detrimental for the amplitude of swab and surge pressures [20]. However when the drill-string is in cased hole and far above the open hole section, faster acceleration/deceleration will improve tripping speed.

Management of electrical loads on the drawwork motors is an integral part of the Drilling control system (DCS), which typically reduces the commands given by the driller to accommodate the available electrical energy and the required mechanical power. Energy storage will increase the amount of available electrical power, and consequently reduce the operational limits.

2.5.2 Drawwork load during tripping

A theoretical approach to calculate the draw work load can be split into four parts:

1) **The load applied by the traveling equipment:**
   The top of string force applied to the traveling block, depends on materials and dimensions (mass) of the drill string, hydrostatic forces (the string is submerged in drilling fluid which is much heavier than water and causes buoyancy), mechanical friction and hydrodynamic forces (due to drilling fluid circulation). The top of string force will evidently depend on the length of the drill string, changing through the tripping process, and to some extent the compression of the drill string [21]. The sum of these forces including the mass of all traveling equipment result in a force, F_{hook} on the traveling block (Figure 2.10), working downwards. The acceleration of the traveling block is determined by F_{hook} , F_{lift}, which is the force from the drilling lines working upwards on the traveling block, and the mass of the drill string, M, as shown in Eq. 2.9.

$$F_{lift} = M\frac{dV_{bolck}}{dt} + F_{hook} \qquad \text{Eq. 2.9}$$

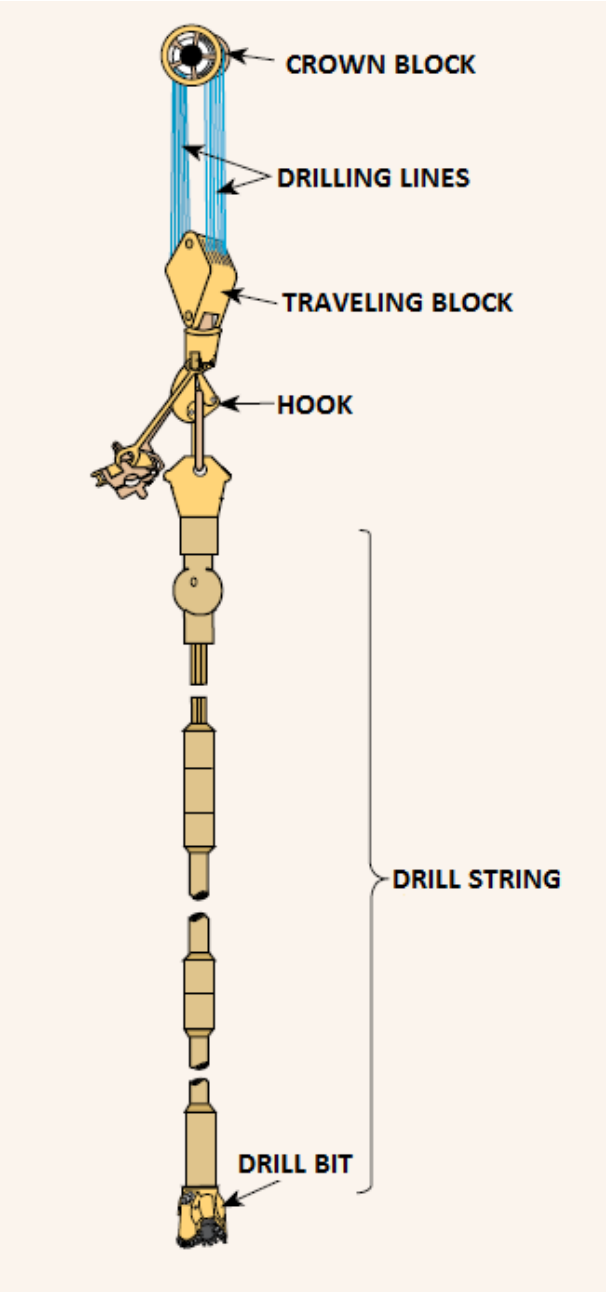

Figure 2.10 - Drill string [32]

2) **The tension on the drill-line on the draw-works side:**

Using pulleys in a block and tackle configuration, the force is reduced as shown by Eq. 2.10, where F_{DW} is the drill-line tension on the draw-works side, F_{lift} is the top of string force, N is the number of line segments extending between the pulleys and η is the efficiency of the pulley system.

$$F_{DW} = \frac{F_{lift}}{N * \eta} \qquad \text{Eq. 2.10}$$

3) **The conversion from tension on the active line to draw-work motor torque:**

Assuming no loss in the pulleys, the torque on the drum can be calculated using Eq. 2.11, where $T_D$is the torque of the drum and r_D is the radius of the drum.

$$T_D = r_D \frac{1}{N}\left(M \frac{dV_{bolck}}{dt} + F_{hook}\right) \qquad \text{Eq. 2.11}$$

The radius of drum depend on how many layers of wire there are on the drum, which changes as the line is spooled in. This means that the ratio between rotational velocity of the drum and the traveling speed of the block is not constant. The rotational speed of the drum ω_D is given by Eq. 2.12 where V_{block} is the velocity of the traveling block.

$$\omega_D = N \frac{V_{block}}{r_D} \qquad \text{Eq. 2.12}$$

There are mainly two types of draw-works; single speed (one gear) and dual gear. For a dual gear draw-work, the gear chosen by the driller will also have an effect on the mentioned ratio.

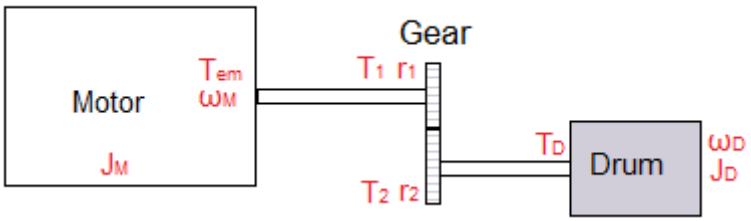

Figure 2.11 - Motor and drum with one gear

Figure 2.11 illustrates a draw-work motor with one gear and drum. Ignoring the mass of the gears and assuming no power loss in the gears, the torques at each end of the gear is given by Eq. 2.13 and Eq. 2.14, where r_1 and r_2 is the radii of each of the gears, J_D is the moment of inertia of the drum, J_M is the inertia of the motor, and T_{em} is the electromagnetic torque.

$$T_1 = T_{em} - J_M \frac{d\omega_M}{dt} \qquad \text{Eq. 2.13}$$

$$T_2 = T_D + J_D \frac{d\omega_D}{dt} \quad \text{Eq. 2.14}$$

$$\frac{r_1}{r_2} = \frac{\omega_D}{\omega_M} = \frac{T_1}{T_2} \quad \text{Eq. 2.15}$$

Eq. 2.15 is the gear ratio. Combining all three equations yields Eq. 2.16 where the electromagnetic torque is expressed as a function of motor speed and block speed. The relation between block speed and motor speed is expressed in Eq. 2.17.

$$T_{em} = \left(J_M + \left(\frac{r_1}{r_2}\right)^2 J_D\right)\frac{d\omega_m}{dt} + r_D \frac{r_1}{r_2}\frac{1}{N}\left(M\frac{dV_{block}}{dt} + F_{hook}\right) \quad \text{Eq. 2.16}$$

$$V_{block} = r_D \frac{r_1}{r_2}\frac{1}{N}\omega_m \quad \text{Eq. 2.17}$$

4) **Control of the draw-work motors:**

There are two main types of draw-works; free fall draw-works and draw works with full velocity control. With free fall draw work, the motors can only lift, and breaking is ensured with by electromagnetic breaking and friction brakes. With full velocity control, the motors operate as generators when breaking, delivering power back to the system which can be handled by breaking resistors or energy storage. Again, there are mainly two types of full velocity control draw works; AC drive with variable frequency drive and four quadrant DC drive with Silicon controlled rectifier.

2.5.3 Electrical load during tripping

The electrical load during tripping can be modelled as a power curve, obtained by combining Eq. 2.18, power consumption in an electric motor, and

Eq. 2.16. Finally the resulting load power is given by Eq. 2.19, where k and J_{eq} is given by Eq. 2.20 and Eq. 2.21. The following assumptions are made: constant drum radius, constant mass of the drill string, no elasticity in the rope or drill string, no loss in the pulleys, gears or drum.

$$P = T\omega \quad \text{Eq. 2.18}$$

$$P = \left(\left(\frac{1}{k^2}J_{eq} + M\right)\frac{dV_{block}}{dt} + F_{hook}\right)V_{block} \quad \text{Eq. 2.19}$$

$$k = r_D \frac{r_1}{r_2}\frac{1}{N} \quad \text{Eq. 2.20}$$

$$J_{eq} = J_M + \left(\frac{r_1}{r_2}\right)^2 J_D \qquad \text{Eq. 2.21}$$

These equations are implemented in a Simulink model, described in Appendix 5, to generate load curves. Parameters for the draw work is based on a datasheet for an AHD-750 drawwork [22], while parameters for the electrical motors is based on GEB22A inductions motors shown in Appendix 6 and summarized in Table 2.2. Parameters such as the force on the hook, F_{hook}, is not given directly in the draw work datasheet, but is calculated by studying the graphs given in the datasheet.

Gear ratio	r_1/r_2	1/10.5
Number of lines	N	12
Drum radius	r_D	1.6m
Drum inertia	J_D	8 kgm2
Motor inertia	J_M	18 kgm2
Number of motors		5

Table 2.2 - Draw-Works parameters

Figure 2.12, Figure 2.13 and Figure 2.14 show load curves for hoisting of three different loads; 45 tons, 270 tons and 630 tons. For the whole tripping process these load patterns will repeat as each segment of the drill string is hoisted. Between each hoist, the hook has to be lowered, which takes around 30 or more seconds [22].

One should note that the calculated load curves do not take into account that the diesel generators preferably use 5-10 seconds to accelerate and supply the given power. If the generators are not capable of delivering this power, the process would be slowed down by the drilling control system. So these curves illustrate what may be achieved when adding an Energy Storage. It is important that the energy storage will mostly be active when the power is rising from zero to constant power. In other words, the ES is not intended to increase the constant hoisting speed, but to allow faster acceleration of the draw work motors.

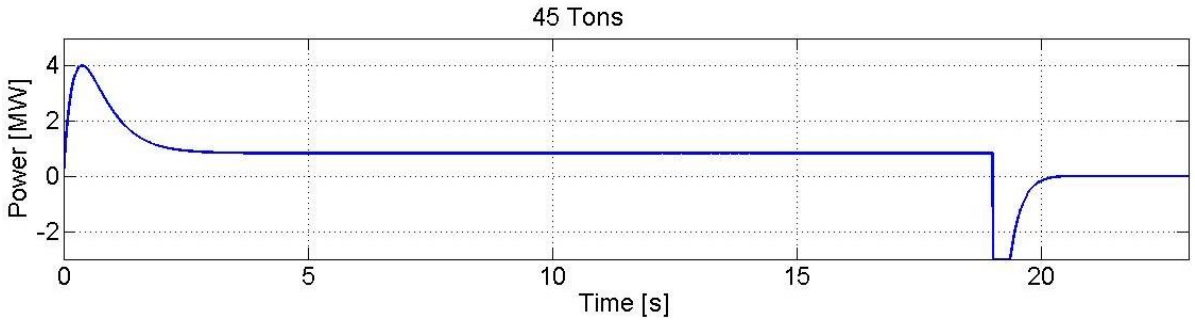

Figure 2.12 - Draw work power, Hoisting 45 tons

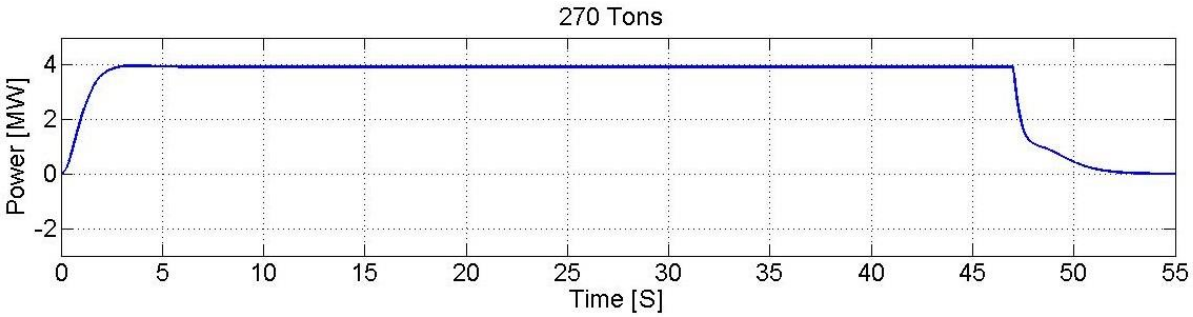

Figure 2.13 - Draw work power, Hoisting 270 Tons

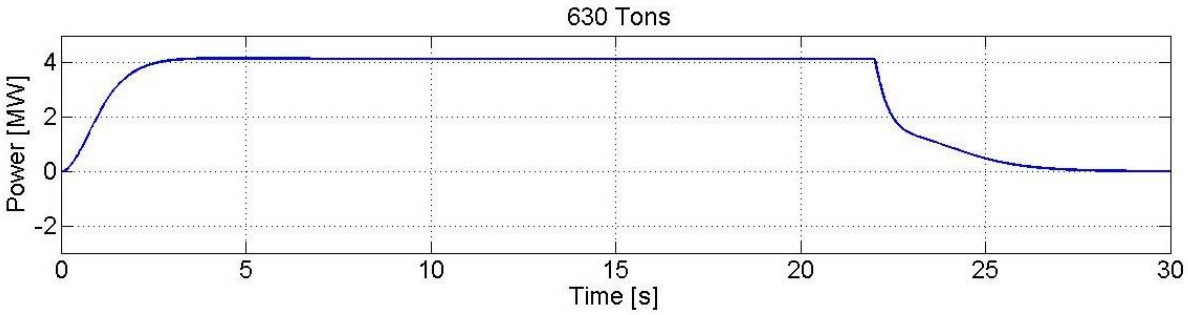

Figure 2.14 - Draw work power, Hoisting 630 Tons

3 Model description

3.1 Load scenario

Modelling the system requires narrowing of the problem to exclude unnecessary calculations and reduce simulation time.

On the basis of section 2.5.3, there are mainly two situations where an ES can allow rapid increase in load. Hoisting of large loads, where the power stabilizes at 4MW, and hoisting of low loads, which has a 4 MW peak followed by lower constant power level. The high load scenario occurs repeatedly during the first half of the tripping operation when the drill string is lifted, while the low load scenario occurs during the second half of the tripping operation, when the empty hook is lifted. As discussed, the ES will deliver energy as the diesels are slowly accelerated. To minimize simulation time, only these time slots will be simulated. For the rest of the cycle, the ES needs to recharge preferably to maximum charge. The time available for recharging is much longer than the time used to discharge, so the recharge current is much lower than the discharge current. Thus recharging of the ES is not considered problematic, hence the discharge of the ES is dimensioning for the size of the ES and converter.

The studied system from Figure 2.2 may consist of several fairly identical DC buses, each with an equal number of generators. How much energy the ES must supply during tripping depends on how many generators are running, and the load sharing between the generators. Each generator has 3.333 kVA rated power, while the load scenarios demands 4MW maximum power, so at least two generators must be running. By splitting the load in half, the model is reduced to only include one generator, which must handle half of the tripping load. The basic assumption is that the rest of the load can be handled by other generators.

Figure 3.1 and Figure 3.2 shows the two load scenarios for the one-generator-model. Figure 3.1 is called the high load scenario, and Figure 3.2 is the low load scenario.

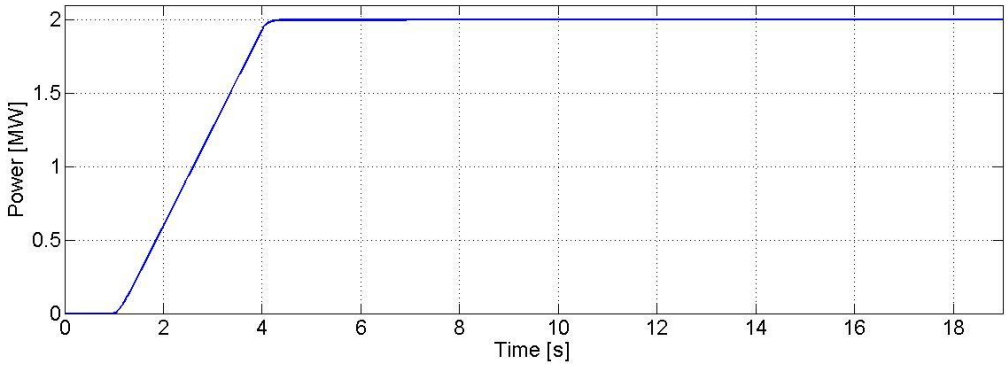

Figure 3.1 - High load scenario

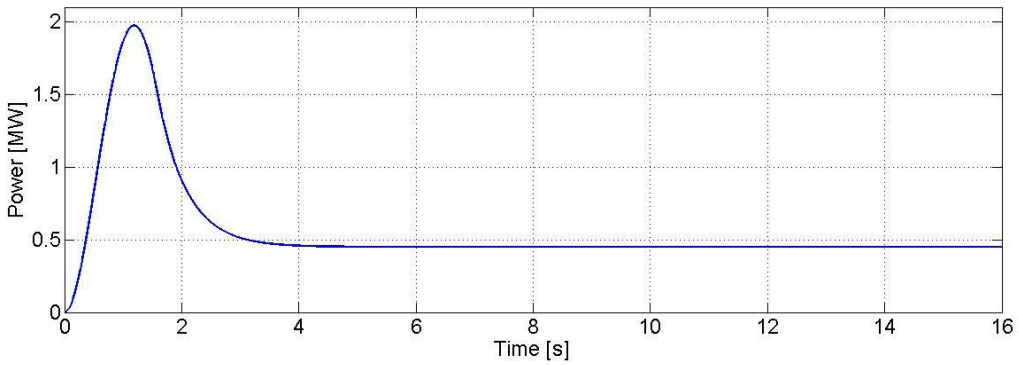

Figure 3.2 - Low Load Scenario

3.2 Diesel engine and generator

The diesel is modelled simply as a first order system (Eq. 3.1) as in ref [23] and [11]. This means that a time constant, T, decides the delay from a set-point is changed to the speed is altered.

$$\frac{1}{Ts+1} \qquad \text{Eq. 3.1}$$

In contrast to an AC system, a DC system allows the diesels to operate at variable speed. In these systems, the diesel is controlled to operate at optimal speed based on the measured load power [24]. For the high-load scenario, the diesel will respond to an almost linear increase in load followed by constant load (Figure 3.1). Based on the diesels optimal speed-power curve (Appendix1), the input reference for the diesel model is increased linearly to 0.65pu for the high load and 0.58pu for the low load. The initial speed is set to zero as this is expected to require more energy from the energy storage than if the diesels were running initially.

The generator is modelled using the built in Simulink model, "Synchronous Machine pu standard" with rotor speed as the mechanical input. Key data for the generator is shown in Table 3.1. The model is a 5^{th} order system with relatively high impedances, given in Appendix1.

Simulink block	Synchronous Machine pu standard
Mechanical input	Speed
Rotor type	Sailent pole
Rated Power	3333 kVA / 3MW
Rated Voltage	690 Vrms

Table 3.1 - Generator model data

The diesel generator model is depicted in Figure 3.3. The field voltage is regulated with a PI controller to keep the dc-bus voltage at 930V. Data for the PI-controller is given in Table 3.2.

Proportional gain	0.8
Integral gain	0.2
Upper saturation limit	3.5
Lower saturation limit	0

Table 3.2 - PI controller parameters

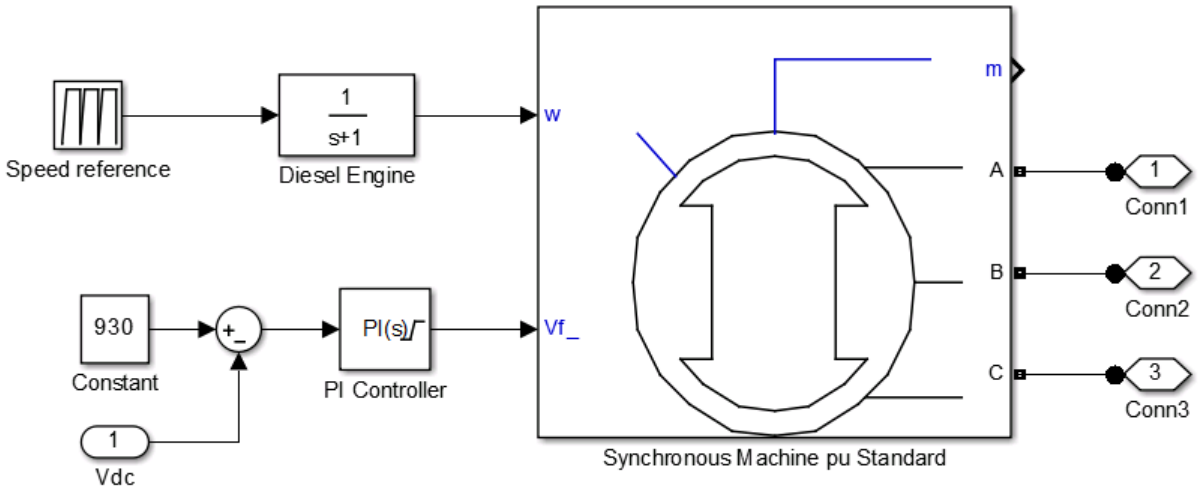

Figure 3.3 - Diesel generator model

The rectifier is modelled as an ideal diode bridge with no losses. A filter is often required on the rectifier output to even out voltage and current. Typically an LC filter is applied. In this model however, the load model is a current source which equals infinite inductance, so there will be practically no current ripple. There is also a capacitor on the converter output which is in parallel with the rectifier output, acting as a filter for the DC voltage.

3.3 Energy storage model

3.3.1 Energy and Power requirements

The power and energy requirements for the ES are decided by the generator and load power. The simulations will show how big the ES needs to be, but an estimation of these values can be done in beforehand with the assumption that the input torque is constant, which makes the generator power proportional to the axial speed. The ES must deliver the difference between the power demand from the load and the power supplied from the generator, as displayed in Figure 3.4 and Figure 3.5.

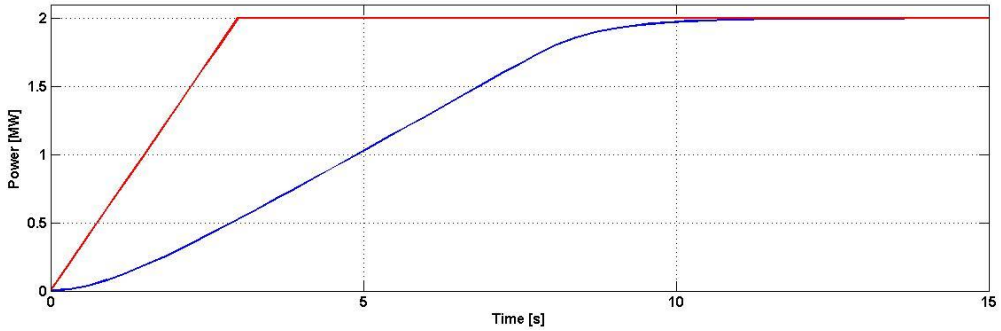

Figure 3.4 - Estimated Load Power (red) and generator power (blue)

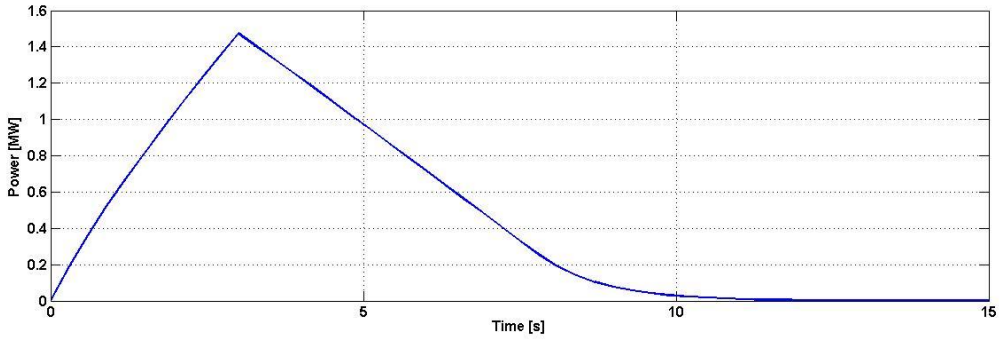

Figure 3.5 - Estimated ES Power

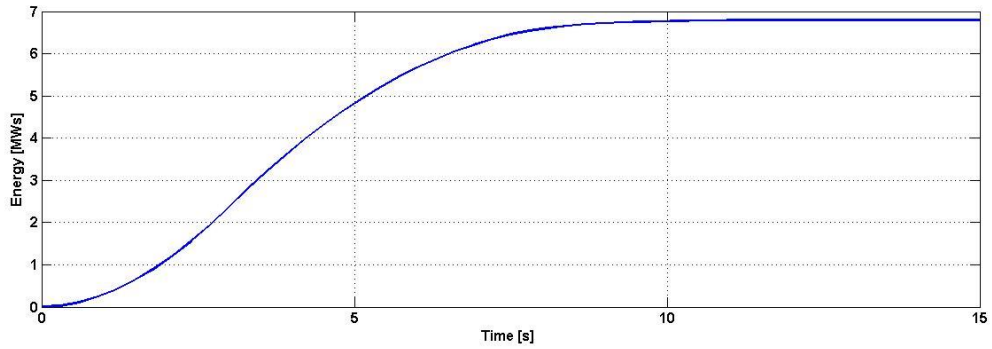

Figure 3.6 - Estimated ES energy

Figure 3.5 shows that the ES in this case is required to deliver 1.5MW maximum power after 3 seconds. Figure 3.6 displays the energy supplied by the ES, and shows that the minimum energy that must be delivered from the ES is 7 MWs. Both the electrolytic- and Supercapacitor ES is modelled as an ideal capacitor in series with a resistor, but due to different limitations and characteristics they have to be studied separately for dimensioning the ES model.

3.3.2 Electrolytic capacitor ES

The electrolytic capacitor ES model is based on data for a 450V HCGW2 series capacitor, which is an aluminium capacitor with etched foil technology that offers high capacitance and

high energy density [25]. Energy stored in a capacitor is given by Eq. 3.2, for a capacitor with capacitance, C, which discharges from maximum voltage, V_{max} to discharge voltage, V_{min}.

$$W_c = \frac{1}{2} C \left({V_{max}}^2 - {V_{min}}^2 \right) \quad \text{Eq. 3.2}$$

Vrated	450 V
Terminal allowance current	100 A rms
Ccap	25 mF
ESR (100Hz)	16mOhm
Case diameter	90mm
Case hight	234mm

Table 3.3 - HCGWW22W253YF234 capacitor

The ES capacitor bank consists of several capacitors connected in parallel. With a given voltage of 450V, the maximum energy capacity of the ES is decided only by the total capacitance of the bank given by Eq. 3.3, where n is the number of capacitors, and C_{cap} is the capacitance of one capacitor.

$$C_{bank} = n \cdot C_{cap} \quad \textbf{Eq. 3.3}$$

The modelled ES is dimensioned to have 14.4 MWs which, based on the calculations in section 3.1, is more than available. This will allow the energy storage to be operational even if it is not fully loaded. To calculate the corresponding capacitance, one must also decide the discharge voltage of the capacitors. A low discharge voltage will result in higher ES current and large current ripple in the converter. The modelled ES is dimensioned to have a discharge voltage of 225 V. Using Eq. 3.2 the total capacitance of the ES is 189.63 F, which requires 7585 capacitors.

With 7585 capacitors in series, the total ESR of the ES will be reduced to 2μΩ which is very small. The maximum allowed current in the capacitors increases when they are put in series to 758.5 kA, which is far more than needed to deliver 1.5MW. So for the electrolytic capacitor ES, the current is not limited by what the capacitors can handle but by the IGBTs in the converter. Figure 3.5 shows that the ES has to deliver 1.5MW after using 2.5MWs from the storage, which for the 14.4MW ES correspond to a voltage drop from 450V to 420V(Eq. 3.2). Delivering 1.4MW at 420V requires a current of 3336A. A slower response from the generator would, however, require the ES to supply closer to 2MW. Also considering that the ES might not be fully loaded, the ES is modelled to be able to supply 2MW at 250V, which requires a current of 8000A.

Modern IGBTs can handle up to 2000A with continuous switching. This can be solved by using 4 IGBTs in parallel, or using 4 converters in parallel. The first alternative is simple and cheap, but dividing the ES on different converters opens for a few opportunities. With two or more converters, the ripple current can be reduced by operating the IGBTs with 180 degree

phase shifted switching signals. As seen in Figure 2.2, the system consists of several buses. Dividing the ES into multiple autonomous modules, allows more flexibility in location of the ES, increases the redundancy of the system, and might ease the current requirements for the DC-bu.In the model, the ES is split into four separate modules, with their own converter. Data for each of the modules is summarized in Table 3.4. To decide volumetric energy density, the volume of the ES is calculated using a stacking factor of 60% which takes into account that the capacitors are circular, and leaves room for cables and cooling.

Total Cap	47.425 F
Number of Capacitors	1897
ESR	8.434 μΩ
Voltage	450 V
Energy stored (450V-225V)	3.6 MWs
Energy stored (450V-0V)	4.8 MWs
Max Power (450V)	0.9 MW
Min Power (225V)	0.45 MW
Volume (stacking factor 0.6)	18.83 m3
Volumetric Energy density	70.81 Wh/m3

Table 3.4 - Electrolytic ES module

3.3.3 Supercapacitor ES

The Supercapacitor ES model is based on data from Table 3.5 for a Maxwell capacitor module [26]. This module consists of 48 cells of 3000 F in series, with a total rated voltage of 125V. Connecting four of these modules in series gives a total voltage of 500 V. The maximum instantaneous current of this capacitor is 1900A, but due to thermal issues, the capacitors can only handle a 240A rms current over time. The rms current can be estimated, using the ES power from Figure 3.5 and assuming constant ES voltage of 400V. Figure 3.7 shows the estimated current for the first 15 seconds of the 2MW scenario. The RMS current for the whole tripping cycle also includes recharging of the ES, which is done between the load increases. So the recharge time depends on the weight of the drill string, as described in section 2.5. The charge that needs to be recharged is found by integrating the current in Figure 3.7. 17000As is charged and discharged over 50 seconds resulting in a RMS-current of 680 A. As for the electrolytic capacitor ES, the Supercapacitor ES will consist of modules capable of delivering 2000A, which requires three Maxwell capacitor modules in parallel.

Rated Capacitance	63 F
Max ESR	18mOhm
Rated Voltage	125 V
Maximum Current	1900 A
Max RMS Current	240 A
Energy Capacity (125-0V)	0.504 MWs
Volume (approx.)	0.133 m2
Specific Energy	2.3 Wh/kg

Table 3.5 - Maxwell 125V Heavy Transportation Module

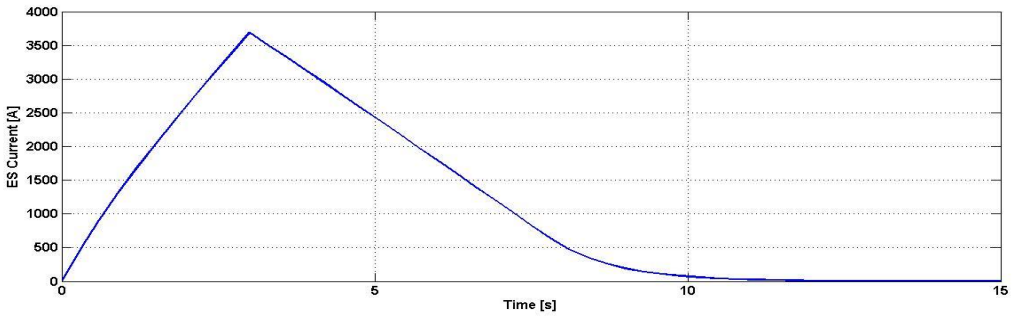

Figure 3.7 - Estimated ES current

To meet the same requirements as with electrolytic capacitors in terms of power capacity, the ES is split in-to four parts, with four separate converters. Each part consists of three parallel strings, where each string has four capacitors (from Table 3.5) in series. The resulting data for the 12 capacitor module is given in Table 3.6.

Rated Capacitance	47.25
Max ESR	24mOhm
Rated Voltage	500 V
Maximum Current	5700 A
Max Continuous Current	720 Arms
Energy Stored (500-0V)	5.906 MWs
Energy Stored (500-225)	4.71 MWs
Volume (approx.)	1.6m3
Volumetric Energy density	1025Wh/m3
Energy density	2.3Wh/kg

Table 3.6 - Supercapacitor Module

3.4 DC-DC Converter

3.4.1 Modelling and dimensioning

As discussed in section3.3, the model will include four identical DC-DC converters. The ES side voltage will range from 500-225V, so it will always be lower than 930V. A four quadrant converter is therefore unnecessary, but a two-quadrant converter is required to allow for bidirectional current flow.

The converter will operate as a boost converter during discharge of the ES, and buck converter during recharge. The ES power is higher during discharge so the converter is dimensioned as a boost converter, while the recharge mode has to be flexible enough to accommodate itself to these selections [7]. Using Eq. 2.6 and Eq. 2.7 with a voltage ripple of 0.2% and current ripple of 3%, gives the inductance and filter capacitance values given in Table 3.7. A fairly high capacitor is chosen to also be able to filter the output voltage from the rectifier. Both the capacitor and inductance are modelled as ideal components. The IGBTs and diodes are modelled as almost ideal components, with parameters given in Table 3.7. Switching frequency in these kinds of converters is typically 2.5-5 kHz. Switching losses

are not considerable in this model, and higher frequency gives faster response time and more accurate control, so the switching frequency is set to 5000Hz.

Inductance, L	1.82mH
Bus-side capacitor, C	0.1 F
Switching frequency, fs	5000 Hz
IGBT/Diode internal resistance	1mΩ
IGBT/Diode, snubber resistance	10^5Ω
IGBT/Diode, capacitance	Infinite

Table 3.7 - Converter Parameters

The converter model is depicted in Figure 3.8. In addition to the power circuitry, the model includes a control system with two loops referred to as “Voltage Control” and “Current Control”.

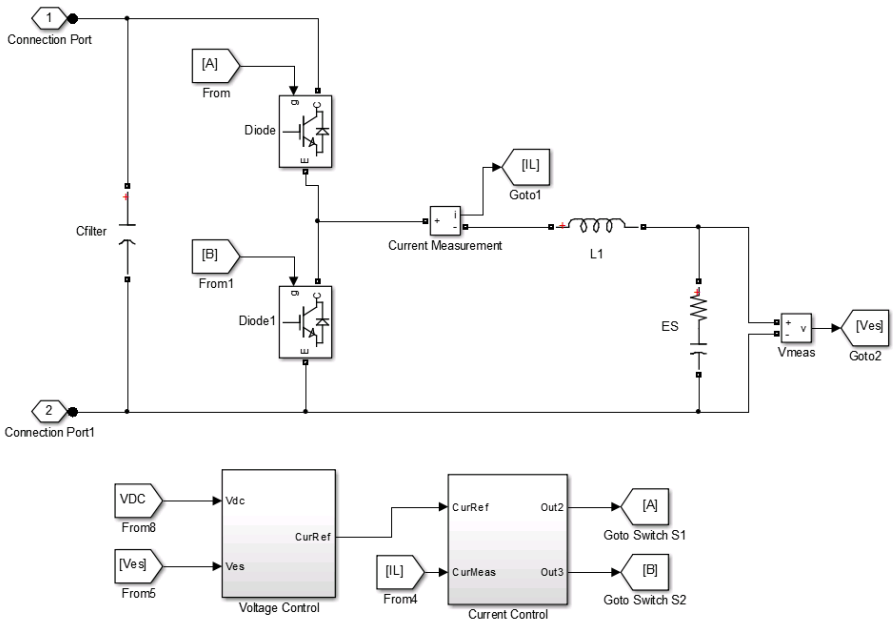

Figure 3.8 - Converter Model

3.4.2 Voltage Control

The voltage control (VC) decides the inverter current, based on the measured DC bus voltage and ES voltage. The direction of the output current reference decides if the ES is charging or discharging. The VC depicted in Figure 3.9 does not handle recharge of the ES as this is not relevant for the described load scenarios.

During normal operation of the VC, the bus voltage is compared to a reference voltage of 920V, and the deviation is input for the PI regulator. The reference voltage is set lower than the nominal bus voltage to ensure load sharing between the ES and generator. But if the measured ES voltage falls below the set discharge voltage of 225V, the deviation signal is set to zero so that the ES stops discharging.

The voltage control also limits the output current reference, so that it will not exceed 2000 A in any direction. In the start of the simulation, before any load current is applied, both negative and positive current reference is allowed to insure that the bus voltage stabilizes. But after 2 seconds, the output is limited to only allow discharging of the ES, so that the ES will not start to recharge immediately as the generator is able to supply the load singlehandedly. One should note that the current is defined as positive when the ES is charging, so in the simulations the current reference will mostly be negative.

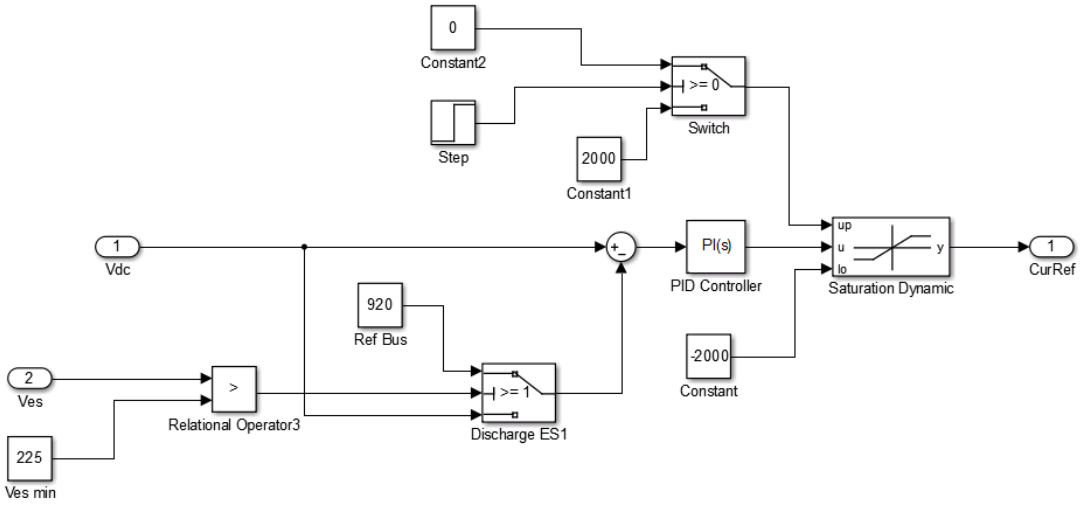

Figure 3.9 - Voltage Control

3.4.3 Current control

The current control (CC) takes a reference signal from the VC, and decides the gate signals for the IGBTs. The inverter current is measured in the inductor on the ES side of the converter (Figure 3.8). The deviation between this measured current and the reference current is input for the PI controller, while the output of the PI-controller is the duty cycle for the switches. The duty cycle is compared to a tri-wave signal (PWM), which gives the rectangular gate signal for switch A. The gate signal for switch B is the opposite of switch A, as long as current is flowing in the converter.

The CC also includes a mechanism for disconnecting the ES entirely when the current reference is zero. This prevents potential ripple currents when the ES is not supposed to interact with the rest of the system.

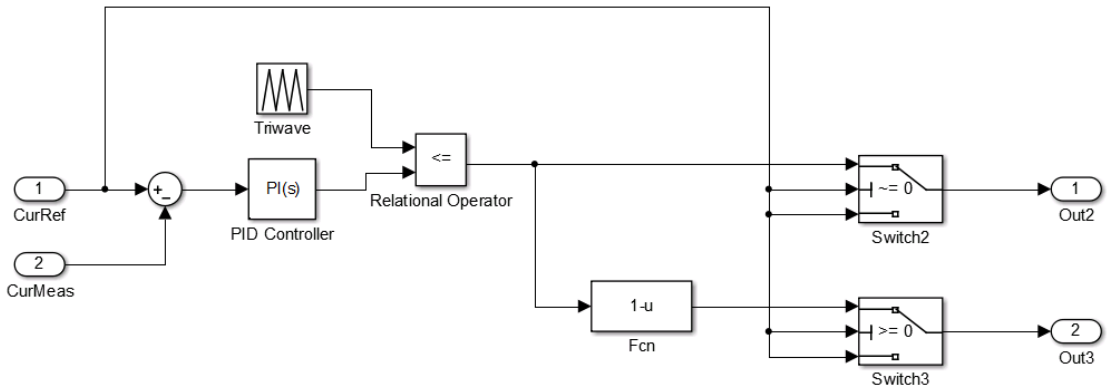

Figure 3.10 - Current Control

3.5 Load model

The load model (Figure 3.11) consists of a current source which is connected in parallel with the rectifier and ES. This model ensures that the load power corresponds to the load curves described in Figure 3.1 and Figure 3.2. The load curves are generated in separate subsystems depicted in appendix 5. The load power is divided by the measured voltage to get the load current. To avoid circle references, a transport delay block is added, delaying the measured voltage signal by 1ms. This also means that the load power will not be entirely constant, which is more realistic. The saturation block in Figure 3.11 is there to ensure that dividing with zero is avoided.

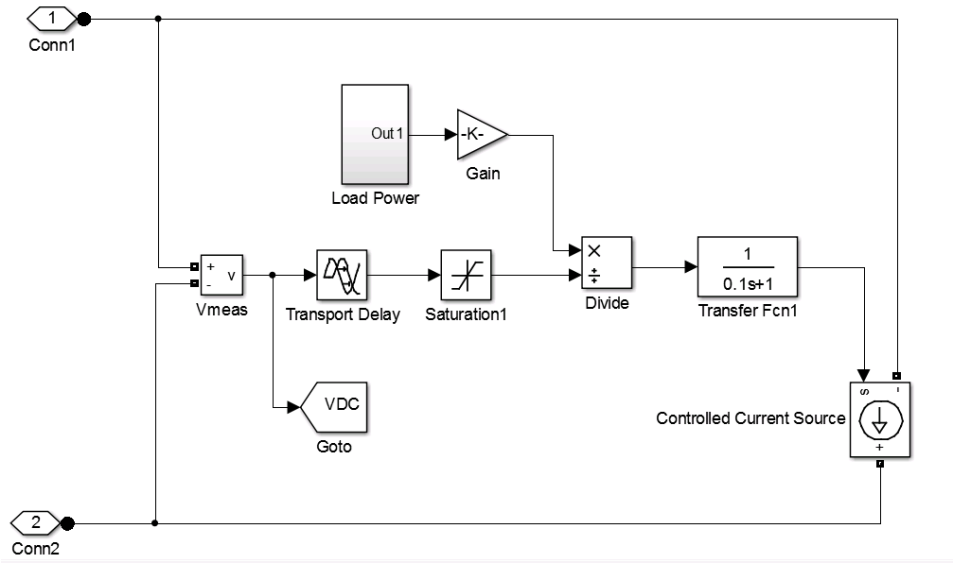

Figure 3.11 - Load Model

3.6 Simulation Set-up

The complete model is depicted in Figure 3.12, a bigger version of this figure is found in appendix 2. As discussed above, there are two alternative energy storages; supercapacitor and electrolytic capacitor. There are also two load scenarios; high- and low load. Consequently four simulations are run. The simulation time is set to 16 seconds for the low load simulation and 19 seconds for the high load scenario. In the start of the simulation, the ES will supply the load and maintain the bus voltage. The simulation starts with no load for one second, so that it can reach steady state before the load starts increasing.

The model (Figure 3.12) consists of elements from two different Simulink toolboxes. The signal part of the model is built using basic Simulink elements, while the power circuit is built with elements from the SimPowerSystem toolbox. The power circuit is solved using the parameters from Table 3.9, and converted to equivalent Simulink state-space equations [27]. These equations are solved using the configuration parameters given in Table 3.8.

Solver	Dormand-Prince
Step-size	Variable step
Relative tolerance	1e-3

Table 3.8 - Simulink Configuration Parameters

Simulation type	Discrete
Solver type	Tustin
Sample time	5e-3 s

Table 3.9 - Powergui Parameters

Most of the parameters in the model are defined in a separate Matlab script found in appendix 3.

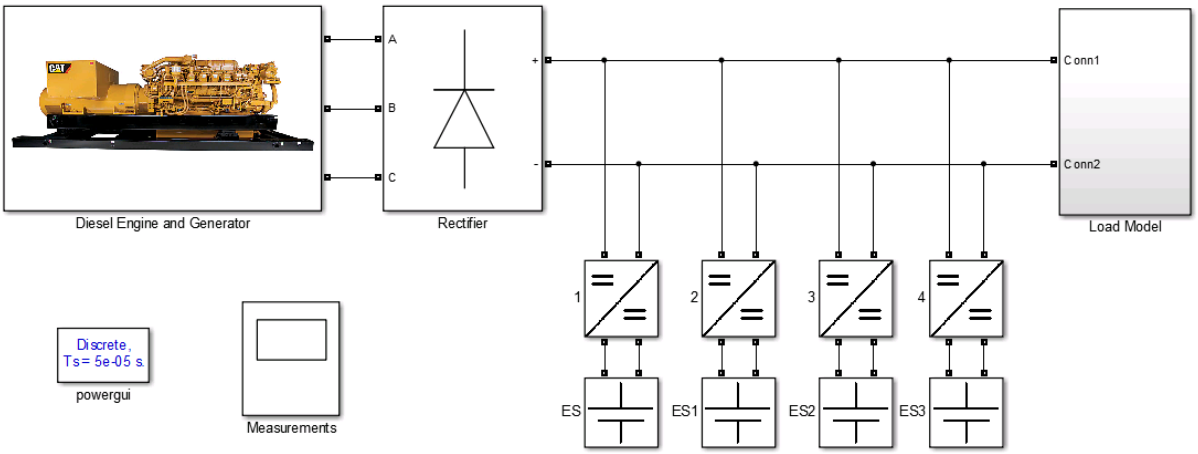

Figure 3.12 – Simulink Model

4 Results

4.1 Electrolytic Capacitor ES with high load

For the high load scenario, the load power is given by Figure 3.1. The reference speed for the diesel rises linearly from 0 to 0.65pu over 7.8 seconds. The ES consists of four electrolytic capacitor models, described in Table 3.4.

The simulation results are shown in Figure 4.1-Figure 4.6 and Table 4.1. RMS current, energy used and efficiency is calculated as described in appendix 4.

Minimum ES voltage	278.6 V
Maximum current in one module	1622 A
Max ES power	1.94 MW
ES operative time interval	8.18 s
Energy loss in capacitor, one module	85.192 Ws
Charge difference, one module	8130 C
RMS current in one module	162.6 Arms
Energy Used	11.84 MWs
Efficiency	99.997%

Table 4.1 - Energy storage key data, Electrolytic Cap ES, High Load

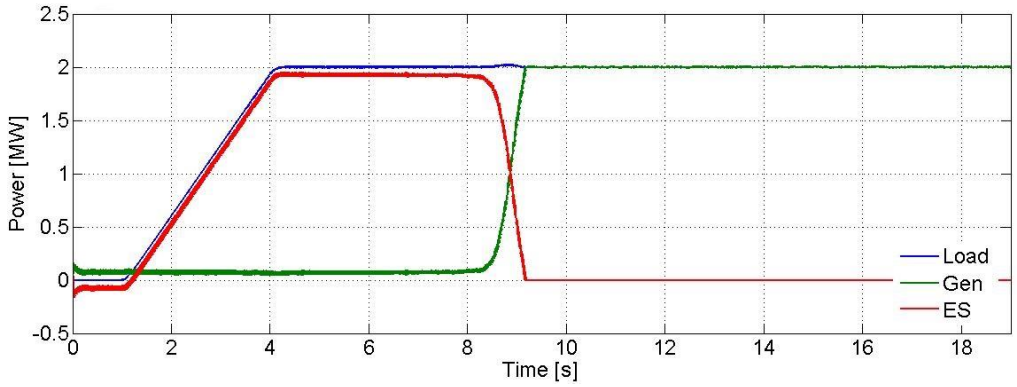

Figure 4.1 - Generator-, load and ES power, Electrolytic Cap ES, High Load

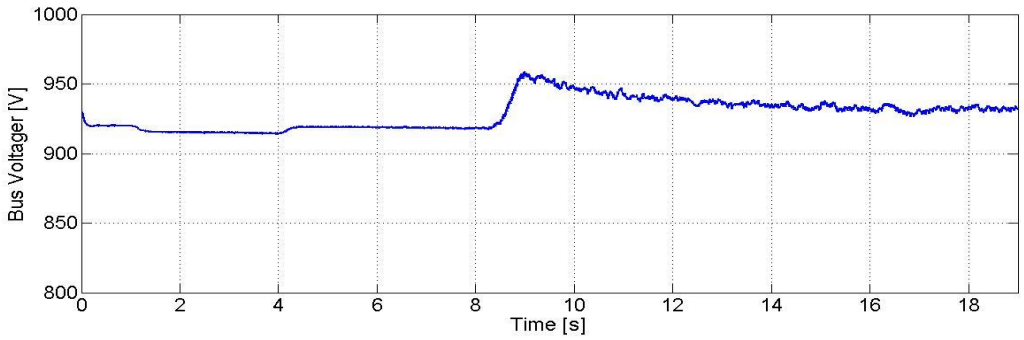

Figure 4.2 - Bus Voltage, Electrolytic Cap ES, High Load

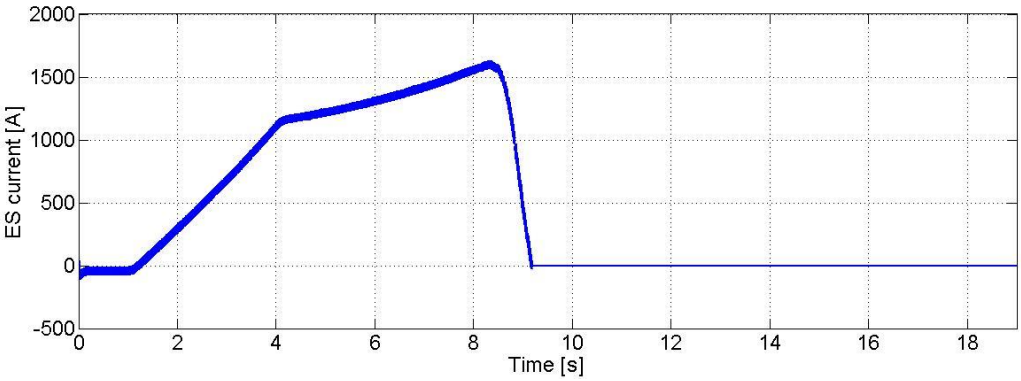

Figure 4.3 - ES current, Electrolytic Cap ES, High Load

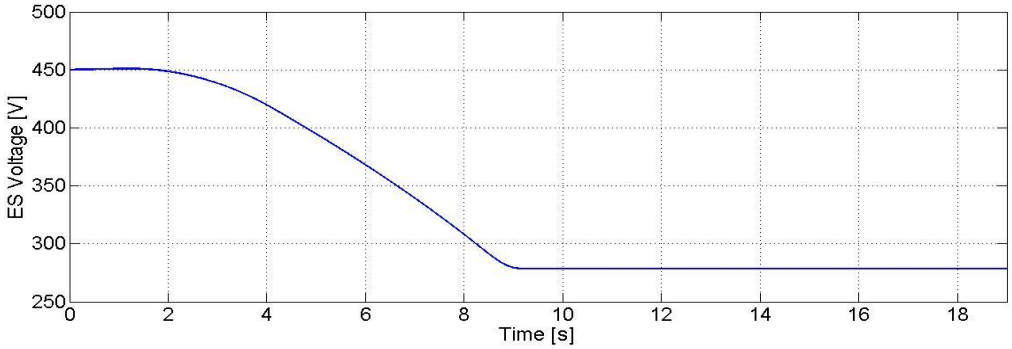

Figure 4.4 - ES Voltage, Electrolytic Cap ES, High Load

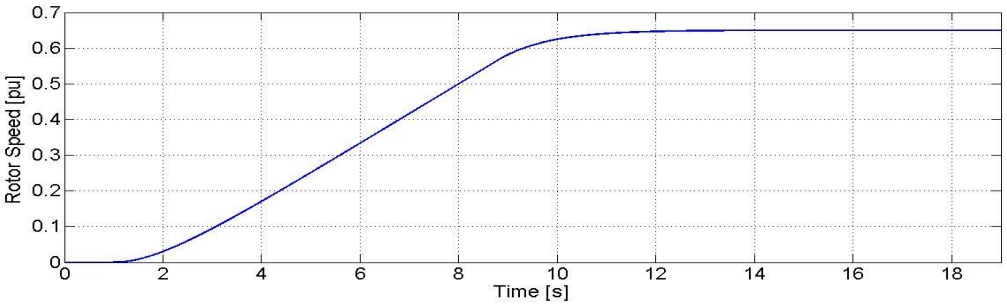

Figure 4.5 - Rotor Speed, Electrolytic Cap ES, High Load

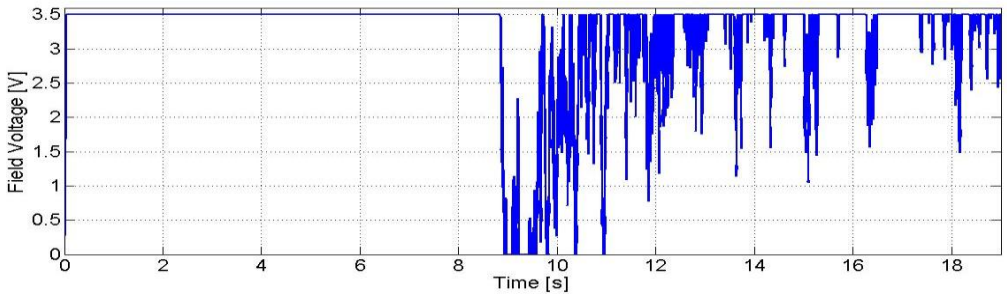

Figure 4.6 - Field Voltage, Electrolytic Cap ES, High Load

4.2 Electrolytic Capacitor ES with low load

For the low load scenario, the load power is given by Figure 3.2. The reference speed for the diesel rises linearly from 0 to 0.55pu over 3.74 seconds. The ES consists of four electrolytic capacitor modules, described in Table 3.4.

The simulation results are shown in Figure 4.7-Figure 4.12, and Table 4.2

Minimum ES voltage	400 V
Maximum current in one module	1114 A
Max ES power	1.918 MW
ES operative time interval	6.75s
Energy loss in capacitor, one module	11.7 Ws
Charge difference, one module	2358 C
RMS current in one module	47.16 Arms
Energy Used	4.04 MWs
Efficiency	99.999%

Table 4.2 – Energy storage key data, Electrolytic Cap ES, Low Load

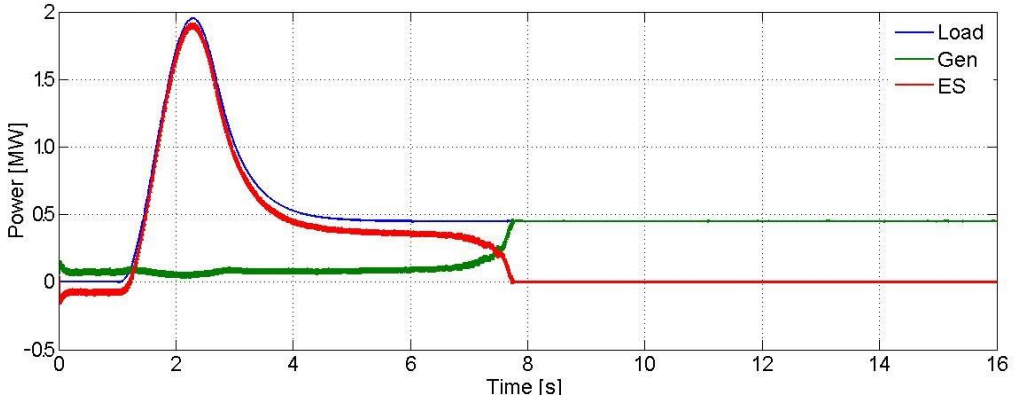

Figure 4.7 – Generator-, load- and ES power, Electrolytic capacitor ES, Low Load

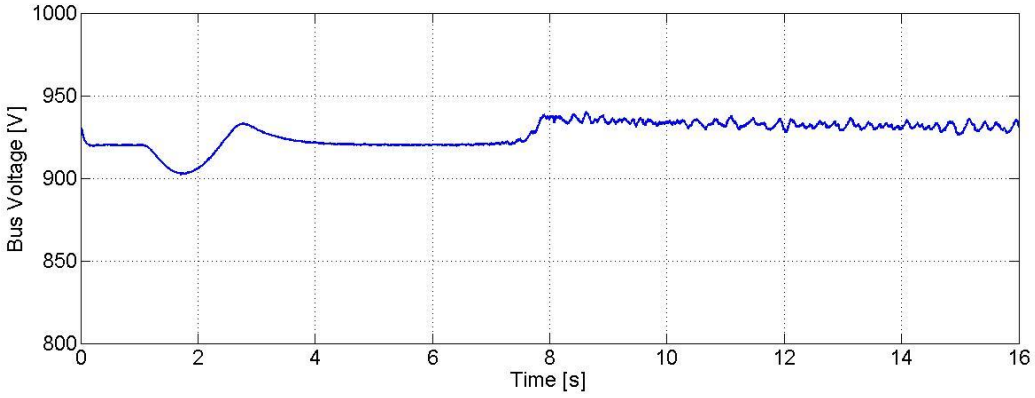

Figure 4.8 - Bus Voltage, Electrolytic capacitor ES, Low Load

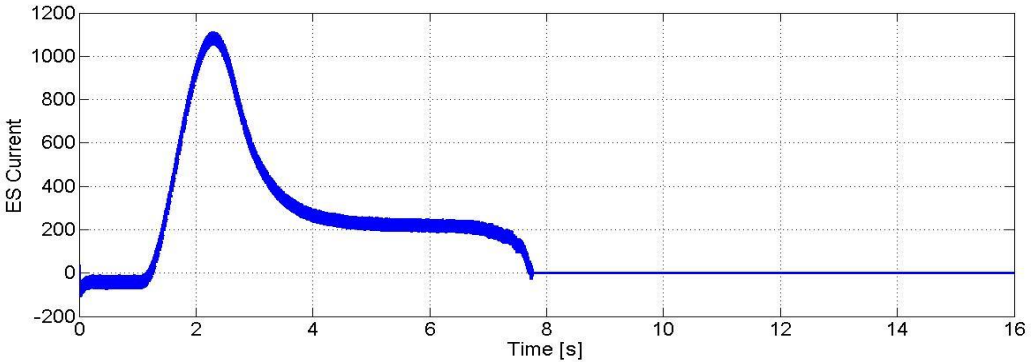

Figure 4.9 - ES current in 1 module, Electrolytic capacitor ES, Low Load

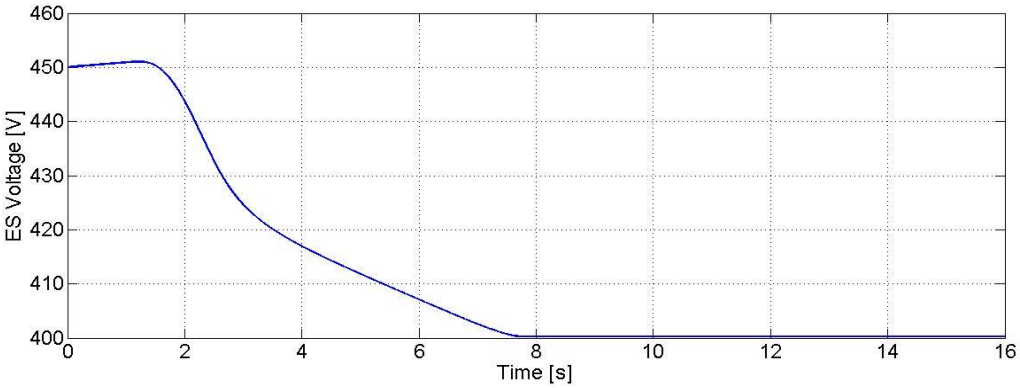

Figure 4.10 - ES Voltage, Electrolytic capacitor ES, Low Load

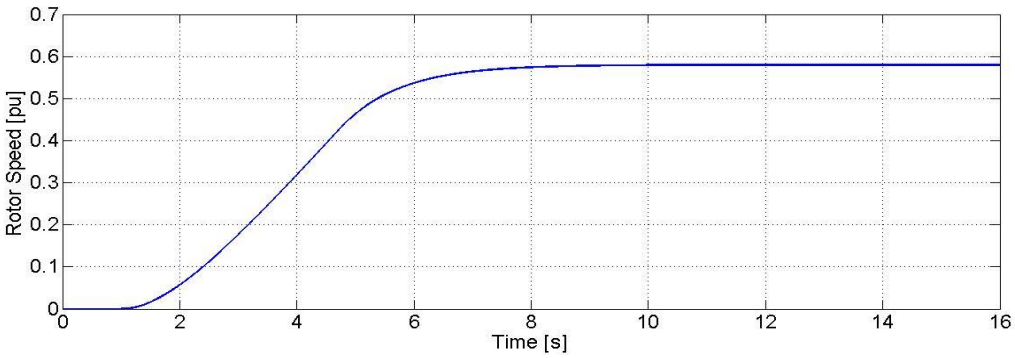

Figure 4.11 - Rotor Speed, Electrolytic capacitor ES, Low Load

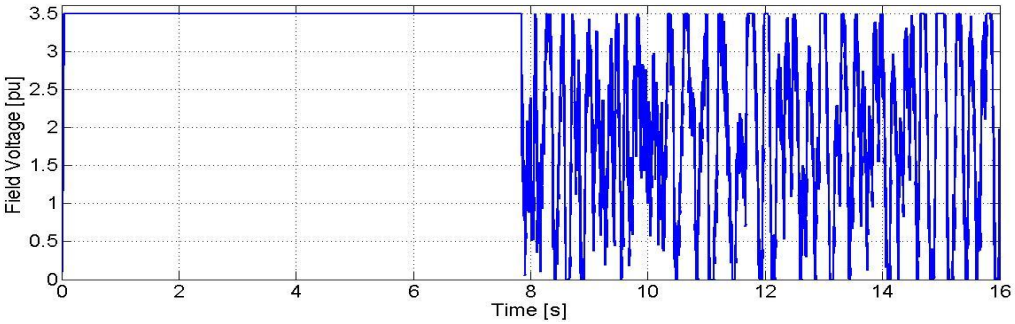

Figure 4.12 - Field Voltage, Electrolytic capacitor ES, Low Load

4.3 Supercapacitor ES with high load.

For the high load scenario, the load power is given by Figure 3.1. The reference speed for the diesel rises linearly from 0 to 0.65pu over 7.8 seconds. The ES consists of four supercapacitor modules, described in Table 3.6.

The simulation results are shown in Figure 4.13-Figure 4.18, and Table 4.3.

Minimum ES voltage	315.5
Maximum current in one module	1502 A
Max ES power	1.94 MW
ES operative time interval	8.1473 s
Energy loss in capacitor, one module	210.14 kWs
Charge difference, one module	7599 C
RMS current in one module	151.98 Arms
Energy Used	14.2 MWs
Efficiency	94.08%

Table 4.3 - Energy storage key data, Super Cap ES, High Load

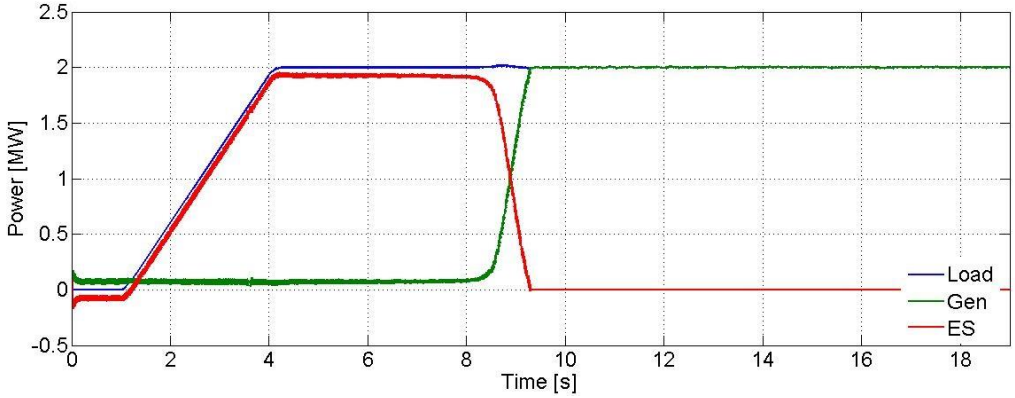

Figure 4.13 - Generator-, load and ES Power, Super Cap ES, High Load

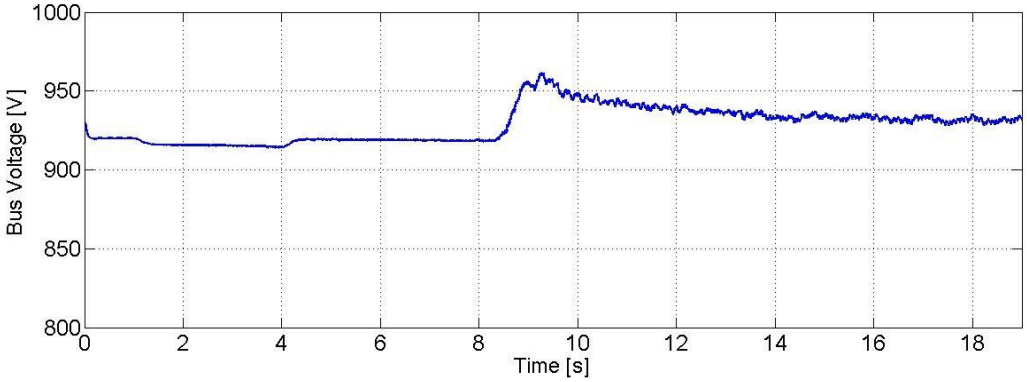

Figure 4.14 - Bus Voltage, Super Cap ES, High Load

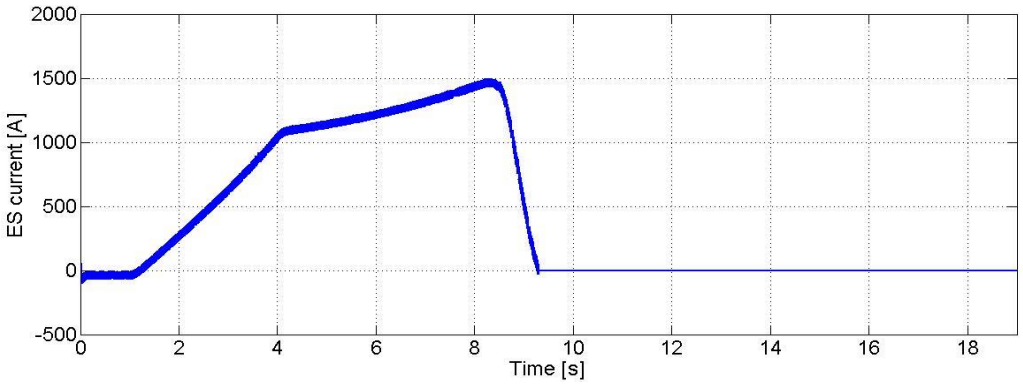

Figure 4.15 - ES Current, Super Cap ES, High Load

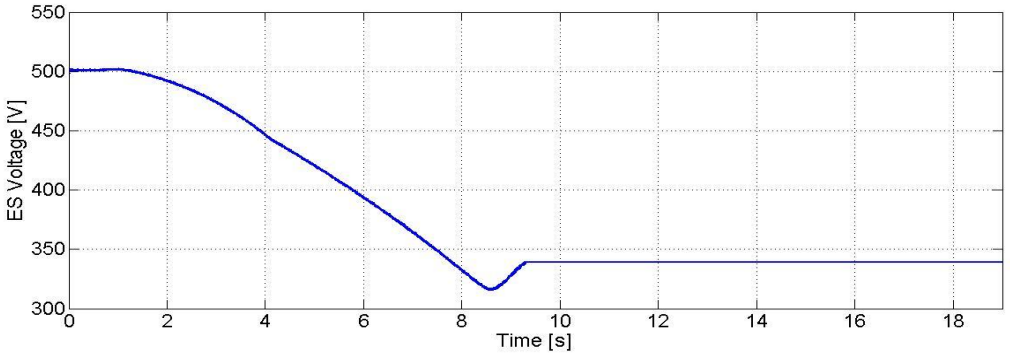

Figure 4.16 - ES Voltage, Super Cap ES, High Load

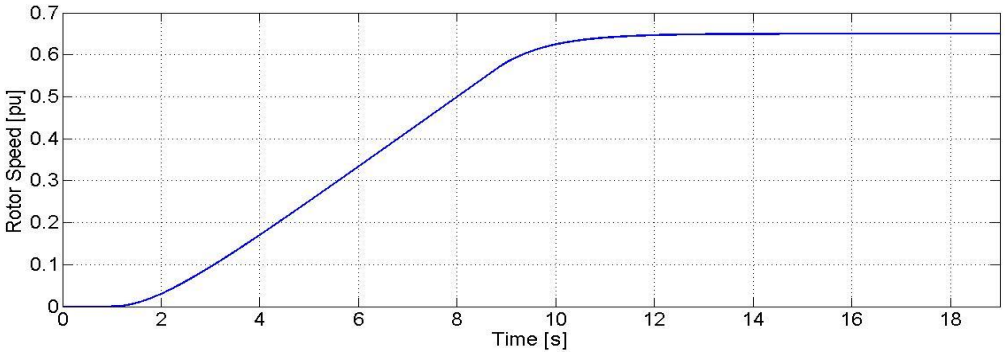

Figure 4.17 - Rotor Speed, Super Cap ES, High Load

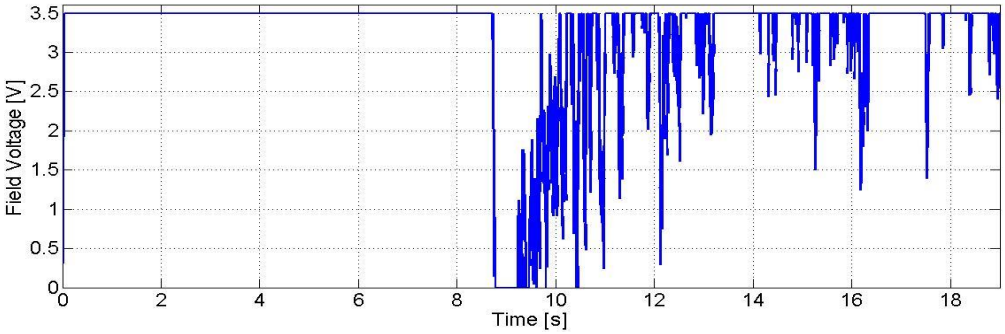

Figure 4.18 - Field Voltage, Super Cap ES, High Load

4.4 Supercapacitor ES with low load

For the low load scenario, the load power is given by Figure 3.2. The reference speed for the diesel rises linearly from 0 to 0.55pu over 3.74 seconds. The ES consists of four supercapacitor modules, described in Table 3.6.

The simulation results are shown in Figure 4.19-Figure 4.24, and Table 4.4.

Minimum ES voltage	454 V
Maximum current in one module	1053 A
Max ES power	1.918 MW
ES operative time interval	6.727 s
Energy loss in capacitor, one module	28.6 kWs
Charge difference, one module	2155 C
RMS current in one module	86.2
Energy Used	4.15 MW
Efficiency	97.24 %

Table 4.4 - Energy storage key data, Super Cap ES, Low Load

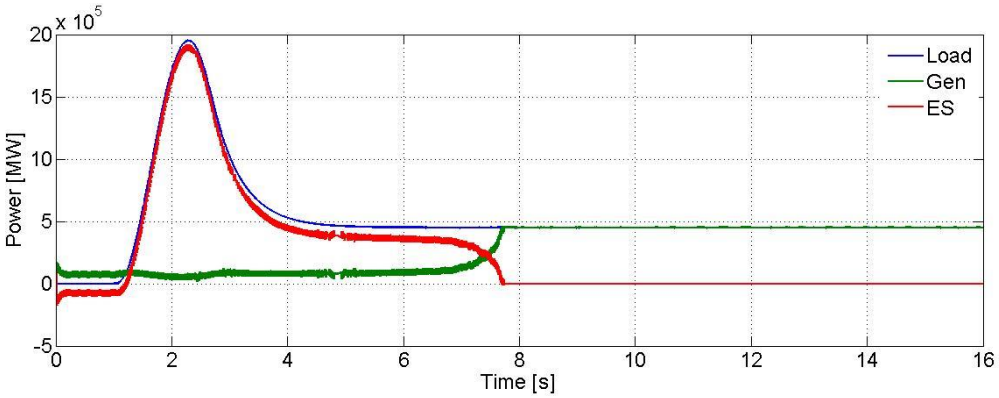

Figure 4.19 - Generator-, load- and ES Power, Super Cap ES, Low Load

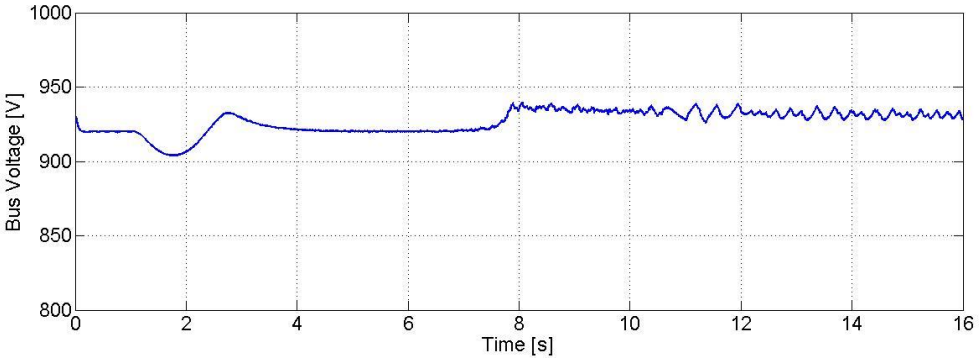

Figure 4.20 - Bus Voltage, Super Cap ES, Low Load

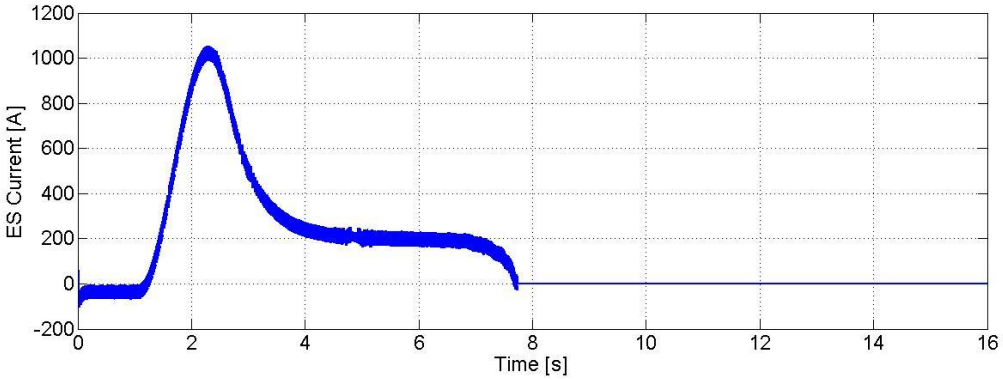

Figure 4.21 - ES Current, Super Cap ES, Low Load

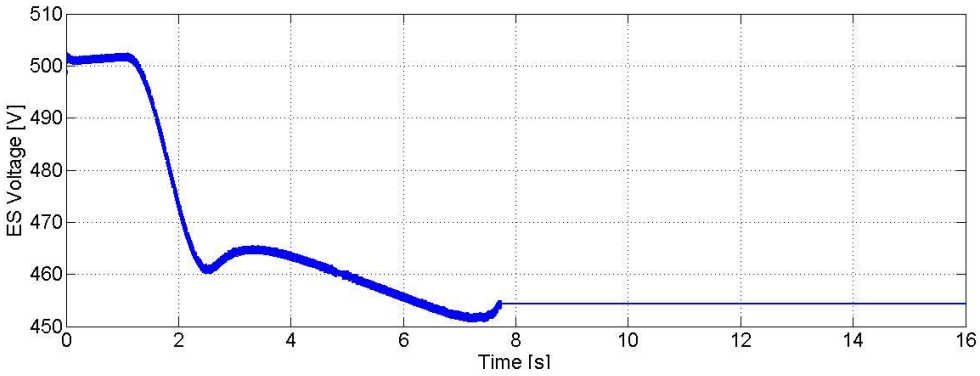

Figure 4.22 - ES Voltage, Super Cap ES, Low Load

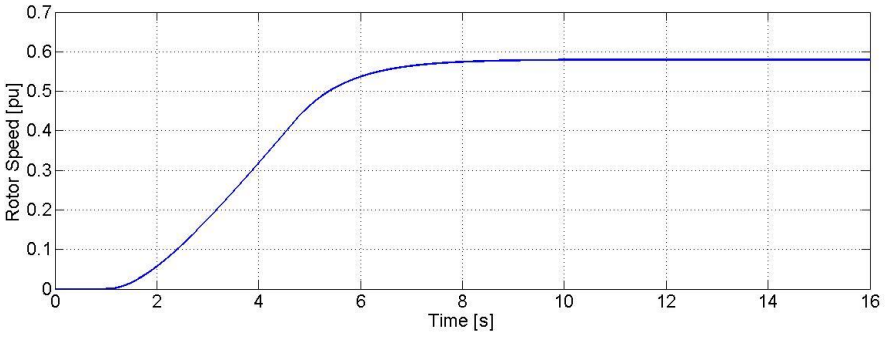

Figure 4.23 - Rotor Speed, Super Cap ES, Low Load

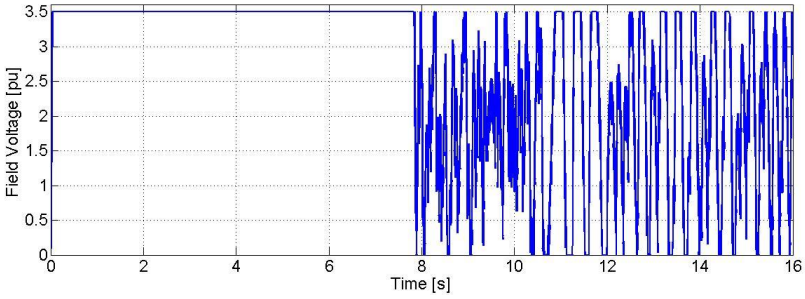

Figure 4.24 - Field Voltage, Super Cap ES, Low Load

4.5 Energy/Power density

The maximum power in the ES during discharge and the energy supplied by the ES can be used to investigate the optimum ratio between energy- and power capacity in the ES. The calculated ratio, defined by Eq. 4.1, for each of the scenarios is shown in Table 4.5.

$$k = \frac{P_{max}}{E} \qquad \text{Eq. 4.1}$$

	$P_{max}[MW]$	$E\ [Wh]$	$k\ [1/h]$
High Load, Electrolytic	1.94	3289	589.84
High Load, Super Cap	1.94	3944	491.87
Low Load, Electrolytic	1.918	1122	1709.45
Low Load, Super Cap	1.918	1153	1663.81

Table 4.5 - Energy and max power in ES

This relation can be used as an indication of what ES technology is best suited for the load scenarios in terms of energy- and power density. Plotting the curve from Eq. 4.2 in Figure 2.3 gives Figure 4.25 with two curves, for the smallest and highest k-value.

$$\frac{P}{m} = \frac{E}{m}k \qquad \text{Eq. 4.2}$$

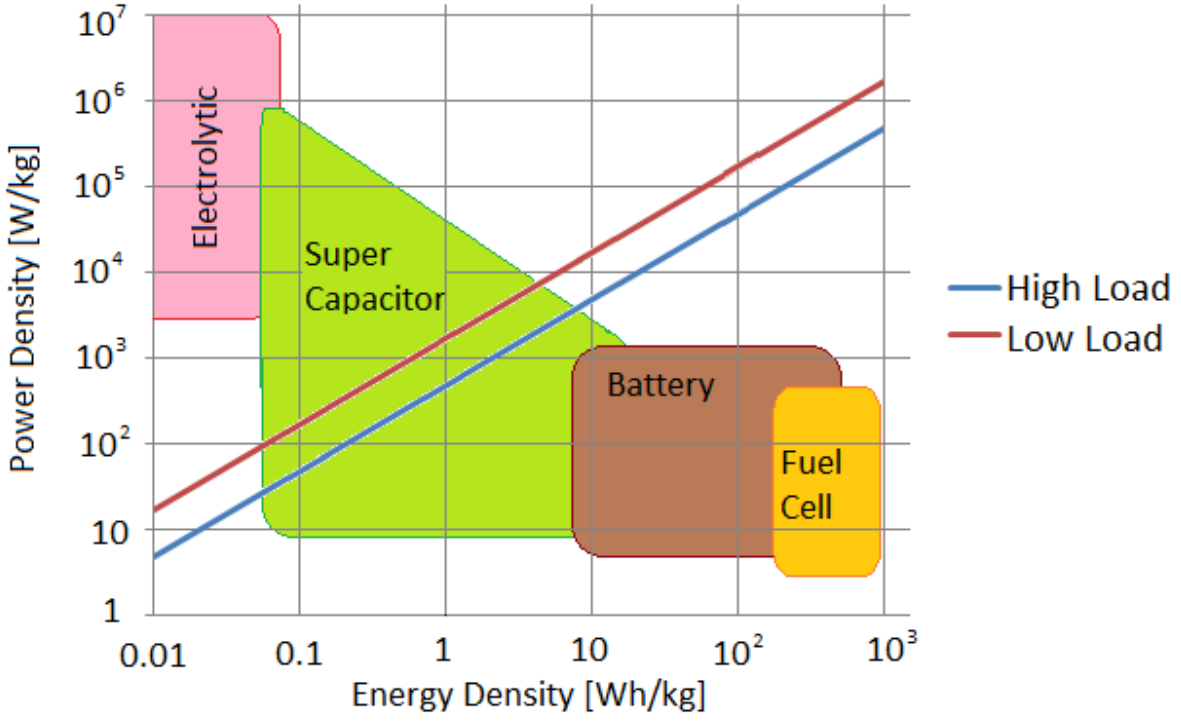

Figure 4.25 - Load power and energy compared to ES technology

5 Discussion

5.1 Explanation of the results

The power graphs (Figure 4.1, Figure 4.7, Figure 4.13 and Figure 4.19) in many ways confirm a successful result. They show that the ES is capable of supplying the load as the generators accelerates. The load start to increase after 1 second, and for all the simulations, the ES is able to follow the increasing load power. The ES is disconnected and the generator takes over after 8.2 seconds for the high load scenario and 6.7 seconds for the low load scenario. This transition is fairly quick, the generators power curve rises from almost zero to full load in 2-3 seconds for all the simulations, even if the rotor speed (Figure 4.5, Figure 4.11, Figure 4.17 and Figure 4.23) rises much slower and the field voltage is constant for the first part of the simulations. This indicates that the diesel engines must supply a rapidly increasing torque (Eq. 2.18), which is not necessarily a problem, but using a different control system with a different load sharing between the generators and ES may have allowed for a smoother transition.

For the first second of the simulation, there is no load. This is necessary to start the simulation with steady state conditions. Due to the nature of the Simulink generator model, there is a small current from the generators supplying the ES in this 1 second interval. This does not affect the results considerably other than the ES voltage being 3-4V higher when the load starts increasing.

The bus voltage indicates if the energy storage is able to supply enough power. For all scenarios (Figure 4.2, Figure 4.8, Figure 4.14, Figure 4.20), the bus voltage stays within 3.5% of rated voltage. The initial voltage is 930 V, but it quickly stabilizes at 920V which is the set point for the energy storage. When the load starts increasing, the voltage drops slightly, before it stabilizes at 920V again during constant load. The voltage curves clearly indicate where the generator takes over and the ES is disconnected. This is indicated by a voltage swell before the voltage stabilizes around 930 V. The voltage swell can be explained by looking at the field voltage (Figure 4.6, Figure 4.12, Figure 4.18 and Figure 4.24), which is at its maximum due to integral wind up. Setting a lower maximum field voltage or resetting the integral in the PI controller could reduce the size of this swag. The bus voltage ripple is higher when the generators are supplying, than when the ES is supplying for all four simulations. Smaller ripple may have been achieved with better tuning of the exciter controller, but the voltage is still within reasonable limits. The fact that the load model is modelled as a current source results in very small ripple in the load current. This makes little room for dynamics between voltage and current, and might result in inevitable voltage ripple.

5.2 Increased tripping efficiency with Energy storage

The time it takes before the generators are able to supply the load without an ES, is also an indication of how much time is saved by using energy storage. As discussed in section 2.5, one cycle of hoisting and lowering takes approximately 45 seconds with low load and 70 seconds with high load. If the time is reduced by 6.7 and 8.2 seconds, the tripping operation efficiency is increased with 11-15%. However, this is only the case when the diesel engines are the limiting factor for how fast the draw work motors can accelerate. It also depends on what kind of diesel engine is used, and the engines' initial state. A diesel with no speed at the start of a load increase will evidently use longer time.

5.3 Supercapacitor vs Electrolytic capacitor

Comparing the Electrolytic capacitor and Supercapacitor, one of the most significant differences is that the Supercapacitor has much bigger losses. As seen in Table 4.3 and Table 4.4, the efficiency of the supercapacitor ES was 94-97.3%, while the efficiency of the electrolytic capacitor ES was more than 99%. This high efficiency can be explained by the fact that the electrolytic capacitors were connected in parallel, and the total resistance of the ES was based on data for single capacitors without including possible resistance in connections between the capacitors. It was also not considered that the resistance depends on frequency and temperature. The Supercapacitors' resistance, on the other hand, was based on data for larger modules of capacitors which gives more realistic results. When evaluating the efficiency/energy loss for the ES, one should also include losses in the converter. These losses were not included in the model as the converter was modelled with almost ideal components. As discussed above, DC-DC converters typically have an efficiency of 97%, which results in a total efficiency of 91-94% for the Supercapacitor ES and 97% for the electrolytic capacitor ES.

The ES voltage cuves (Figure 4.4, Figure 4.10, Figure 4.16 and Figure 4.22) shows that the ES voltage did not reach its lower limit (discharge voltage) for any of the simulations. The lowest ES voltage occurred with electrolytic capacitors and high load which also resulted in the highest ES current (Figure 4.3). Maximum current for all the simulation was below the limit of 2000A, indicating that the ESs could potentially deliver much more power. This is expected, as the dimensioning factor for the Energy storage was the energy capacity, not the power capacity. The fact that the Supercapacitor had an initial voltage of 50V more than the electrolytic capacitors, resulted in lower current for the super capacitors.

When it comes to energy and power density, Figure 4.25 indicates that the Supercapacitor is the best suited technology for the studied loads. The huge power capacity of the electrolytic ES was not utilized. The volume of the Supercapacitors is also smaller than electrolytic ES. One important factor that could reduce mass and weight of the ES would be to increase the voltage level of the ES. But this would set higher requirements to the converter, and if the voltage on the ES is higher than 1000 V, it would be classified as high-voltage equipment with a new set of standards for protection and safety.

6 Conclusion and further work

The simulation results indicate that energy storage can reduce the time it takes to hoist a load by 6.7 seconds for low load and 8.2 seconds for high load. This means that the efficiency of the tripping operation is improved by 11-16%. The energy storage was able to maintain the bus voltage within reasonable limits; confirming that the ES and converter model was able to respond fast enough and deliver the required load power while the diesel generator accelerated. The simulations also answered how much power and energy the ES is required to supply for the given load scenarios. Comparing these results with the power- and energy density for electrolytic- and supercapacitor showed that supercapacitors are the best choice of energy storage to improve a tripping operation.

This thesis has also described how to develop a tool for studying energy storage in dc systems. This model may lay the foundation for further studies.

Further work based on this thesis may include:

- Expanding the model to include more detailed models of diesel engines. This can be used to study how an energy storage can reduce fuel consumption and emissions.
- Building more accurate load models, including frequency converters and induction motors.
- Studying other load scenarios than tripping such as active heave compensations for floating drilling rigs, or using energy storage as backup power.
- Investigating a holistic solution with hybrid ES. Combining batteries or fuel cells with supercapacitors could significantly increase the energy capacity of the ES.
- Studying control strategies for the energy storage, generators and loads to ensure optimal utilization of the energy storage. This may include Power- and Energy management.
- Analysing fault and stability of the system.

References

[1] Rigzone, “How Do Jackups Work?,” 2014. [Online]. Available: https://www.rigzone.com/training/insight.asp?insight_id=339&c_id=24.

[2] K. Sadeghi, “Significant Guidance for Design and Construction of Marine and Offshore strucktures,” 2008.

[3] Il-Yop Chung, Wenxin Liu, Mike Andrus, Karl Schoder, Siyu Leng, David A. Cartes, and Mischa Steurer, “Integration of a Bi-directional DC-DC Converter Model into a Large-scale System Simulation of a Shipboard MVDC Power System,” 2009.

[4] Ole Christian Nebb, Bijan Zahedi, John Olav Lindtjorn, Lars Norum, “Increased fuel efficiency in ship LVDC power distribution systems,” *Vehicle Power and Propulsion Conference (VPPC),* 2012.

[5] Undeland, Mohan, Robins, Power Electronics, John Wiley & Sons, Inc., 2003.

[6] Bijan Zahedi, Lars E. Norum, “Modeling and Simulation of All-Electric Ships With Low-Voltage DC Hybrid Power Systems”.

[7] J. Picard, “High-Voltage Energy Storage: The Key to Efficient Holdup”.

[8] P. W. Parfomak, “Energy Storage for Power Grids and Electric Transportation: A Technology Assessment,” 2012.

[9] D.-J. L.-J. L. Z. C. LiWanga, “Analysis of a novel autonomous marine hybrid power generation/energy storage system with a high-voltage direct current link,” 2008.

[10] S. M. L. E. G. L. G. F. J. M. C. Sergio Vazquez, “Energy Storage Systems for Transport and Grid Applications,” *IEEE TRANSACTIONS ON INDUSTRIAL ELECTRONICS,* Decmber 2010.

[11] V. Ř. Z. K. P. B. J.Leuchter, “Dynamic Behavior of Mobile Generator Set with Variable Speed and Diesel Engine”.

[12] M. Okamura, “A Basic Study on Power Storage Capacitor Systems,” 1995.

[13] T. S. N. U. H. F. Tatsuto Kinjo, “Output Levelling of Renewable Energy by Electric Double-Layer Capacitor Applied for Energy Storage System,” 2006.

[14] R. J. B. Martin Winter, “What Are Batteries, Fuel Cells, and Supercapacitors?,” 2004.

[15] Kapoka.com, “Building an ESR meter for Testing Electrolytic Capacitors,” [Online].

Available: http://kakopa.com/ESR_meter.

[16] M. A. G. L. N. A. Hajizadeh, “Robust control of hybrid fuel cell/energy storage distributed power generation system in weak grid under balanced and unbalanced voltage sag,” 2010.

[17] U. M. A. M. Kisacikoglu MC, “Load sharing using fuzzy logic control in a fuel cell/ultracapacitor hybrid,” *International Journal of Hydrogen Energy,* 2009.

[18] B. Hauke, “Basic Calculation of a Boost Converter's Power Stage,” 2009.

[19] H. A. Shigenori Inoue, “Bi-Directional DC/DC Converterfor an Energy Storage System,” 2007.

[20] B. D. E. W. D. Eric Cayex, “Automation of Drawworks and Topdrive Management To Minimize Swab/Surge and Poor-Downhole-Condition Effects,” 2011.

[21] J. S. J. A. I. S. Robert Wylie, “Instrumented Internal Blowout Preventer Improves Measurements for Drilling and Equipement Optimization,” 2013.

[22] cLink, “Product Data Sheet, Active Heave Drilling Drawworks, AHD-750-5750-63-82-10.5”.

[23] A. K. A. T. I. F. J. F. HANSEN, “Mathematical Modelling of Diesel-Electric Propulsion Systems for Marine Vessels”.

[24] L. E. N. K. B. L. Bijan Zahedi, “Optimized efficiency of all-electric ships by dc hybrid power systems,” *Journal of Power Sources,* 2014.

[25] H. A. ink., “HCGW2 series datasheet,” [Online].

[26] Technologies, Maxwell, “DATASHEET, 125V HEAVY TRANSPORTATION MODULE”.

[27] Matlab, “Simulink Documentation Center,” 2014. [Online]. Available: http://www.mathworks.se/help/simulink/.

[28] Mathworks, “https://www.mathworks.com/products/datasheets/pdf/simpowersystems.pdf,” [Online].

[29] Bijan Zahedi, Ole Christian Nebb, Lars Einar Norum, “An Isolated Bidirectional Converter Modeling for Hybrid Electric Ship Simulations”.

[30] Junhong Zhang, Jih-Sheng Lai, Wensong Yu, “Bidirectional DC-DC Converter Modeling

and Unified Controller with Digital Implementation," 2008.

[31] N. Mohan, Electric Drives, An integrative Approach, 2003.

[32] L. D. Davis, The Blocks and Drilling Line.

[33] G. M. Hajizadeh A, "Intelligent power management strategy of hybrid distributed generation system," 2007.

[34] A. o. a. n. a. m. h. p. g. s. s. w. a. h.-v. d. c. link, "LiWanga, Dong-Jing Leea,Wei-Jen Leeb, Zhe Chenc," 2008.

Appendix 1: Generator and Diesel engine data

Output	S_n	3333 kVA	Standard	IEC60034	
Voltage	U_n	690 V	Marine classification	DNV	
Frequency	f_n	62,5 Hz	Cooling system	IC81W	
Power factor	p.f.	0,9	Ambient temperature	45 ℃	
Current	I_n	2789 A	Cooling water temperature	38 ℃	
Speed	n_n	750 min^{-1}	Installation altitude	1000 m	
Torque	M_n	42,4 kNm	Insulation class	155 (F)	
Winding pitch	2/3	no	Stator Winding Temperature	<= 145 ℃	(R)
			Field Winding Temperature	<= 145 ℃	(R)

Figure A 1 – Generator data

Reactances and time constants				Zn	0,143 Ω		
	unsat.	sat.		unsat.	sat.		
x_d	453,5	436,8 %	x_q	298,3	%	T_{d0}'	3,930 s
x_d'	85,1	59,2 %	x_q'	298,3	%	T_d'	0,738 s
x_d''	48,6	42,8 %	x_q''	59,1	52,0 %	T_d''	0,011 s
x_2	53,3	46,9 %	x_0	15,3	%	T_a	0,104 s
x_{s1}	24,9	21,9 %					

Figure A 2 – Generator reactances and time constants

Tq''=ca.=1.1Td''

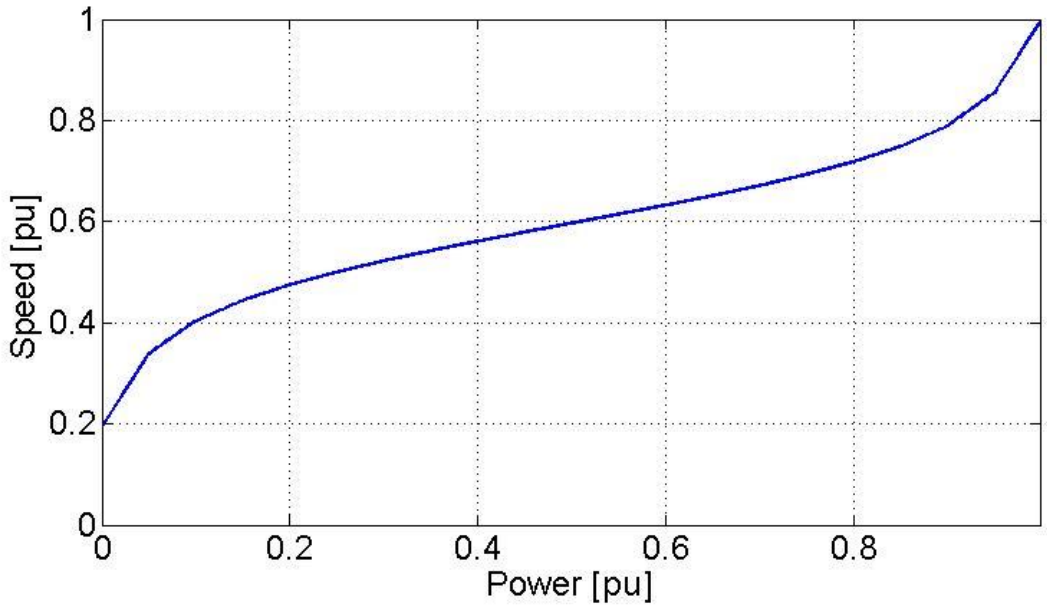

Figure A 3 - Typical optimal speed-power curve for diesel engine

Appendix 2: Picture of Simulink Model

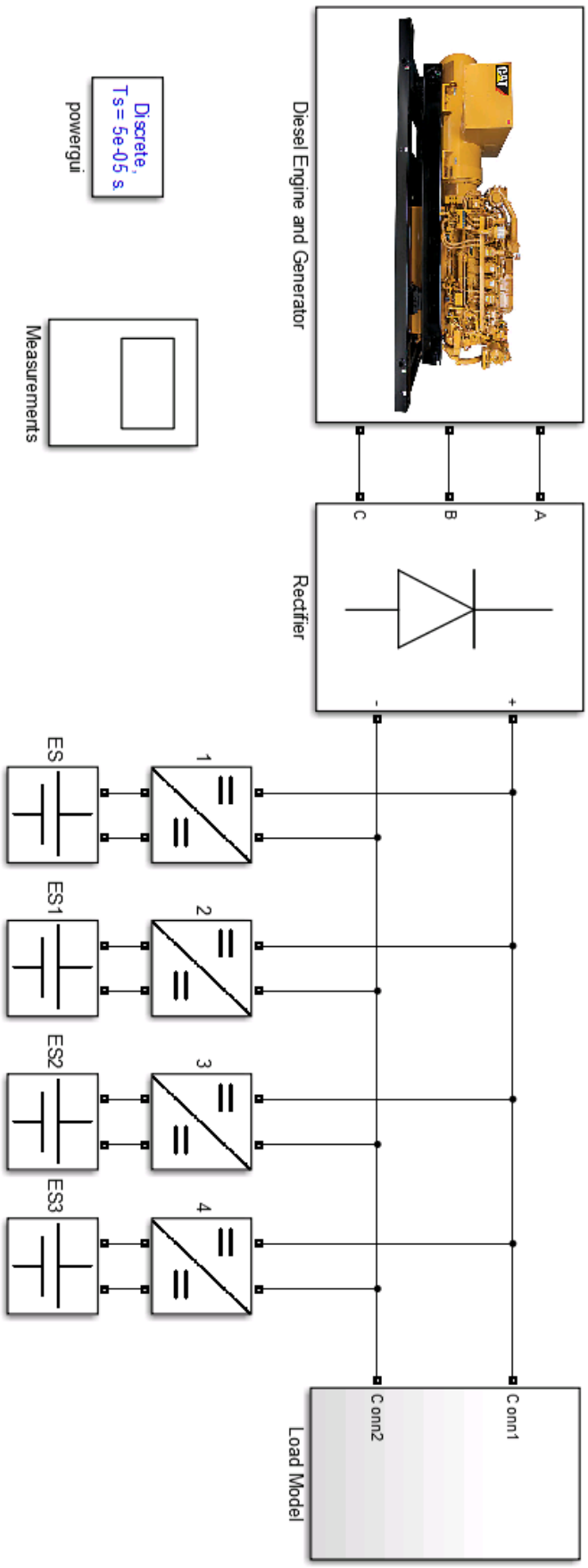

Appendix 3: Model script

```
%Diesel and exciter
nomBV=930;      %Nominal Bus Voltage
T=1;            %Diesel time constant
PVF=0.8;
IVF=0.2;
UVF=3.5;
LVF=0;

%Synchroneous generator
Pn=3333000;     %Nom.Power [VA]
Vn=690;         %Line to line voltage [Vrms]
fsg=62.5;       %Frequency [Hz]
xd=4.535;
xdm=0.851;
xdmm=0.486;
xq=2.983;
xqmm=0.591;
xl=0.249;
Tdm=3.930;
Tdmm=0.011;
Tqmm=1.1*Tdmm;
Rs=0.003;
polepairs=10;

%Electrolytic Capacitor
Ce=47.425;           %Capacitance
Re=8.43437/1000000;  %Resistance
Ve=450;              %Initial Voltage

%Supercapacitor
Cs=47.25;            %Capacitance
Rs=0.024;            %Resistor
Vs=500;              %Initial Voltage

%Converter
L=1/550;
Cf=0.1;
Vcf=930;    %Initial bus voltage

%Current Control
PIC=0.00468;
IIC=0.86262;
freq=5000;           %Switching Frequency
t1=1/freq;
t2=2/freq;

%Voltage Control
PVC=7;
IVC=80;
esSet=920;          %Bus voltage set point for ES
esMin=200;          %Minimum allowed ES voltage
cMax=2000;          %Maximum allowed ES current
```

Appendix 4: Calculating RMS current and efficiency

Calculating the RMS current for one cycle of discharge and recharge of the energy storage is done by measuring how much charge is discharge from the ES. The charge required to recharge the ES equals the charge needed discharge. The rms current is given in Eq.A1, where Q is the measured charge and T is the total time interval including discharge and recharge. For the load studied in section 2, the time T that gives the highest load scenario is

$$I_{RMS} = \frac{2Q}{T} \qquad \text{Eq.A 1}$$

Energy used in the ES is calculated using Eq.A2, where C is the capacitance for one module, and n is the number of modules, which equals 4 for the studied scenarios. The efficiency of the ES is calculated using Eq.A 3.

$$W_{module} = n * \frac{1}{2} C (V_{max}^2 - V_{min}^2) \qquad \text{Eq.A 2}$$

$$\eta = 1 - \frac{W_{loss}}{W_{tot}} \qquad \text{Eq.A 3}$$

Appendix 5: Calculation of load power

The time used to lift the string is adapted by the drilling control system so that peak load is about 4MW, which is close to max rated power of the 5 draw work motors. The power P, is a sum of two addends, resulting in a transient power peak during acceleration, and constant power with constant speed. The weight of the drill string, F_{hook}, will change during the tripping process as segements of the drill string is removed or added. During acceleration of the drill string however, the power also depends on the inertia of the motors and drum, Jeq, which will remain constant. The only variable input for the model is the position of the traveling block. The model for calculating power curves is depicted in Figure A 4. Figure A 5 shows position, speed and acceleration of a traveling block being hoisted 30m of 50 seconds.

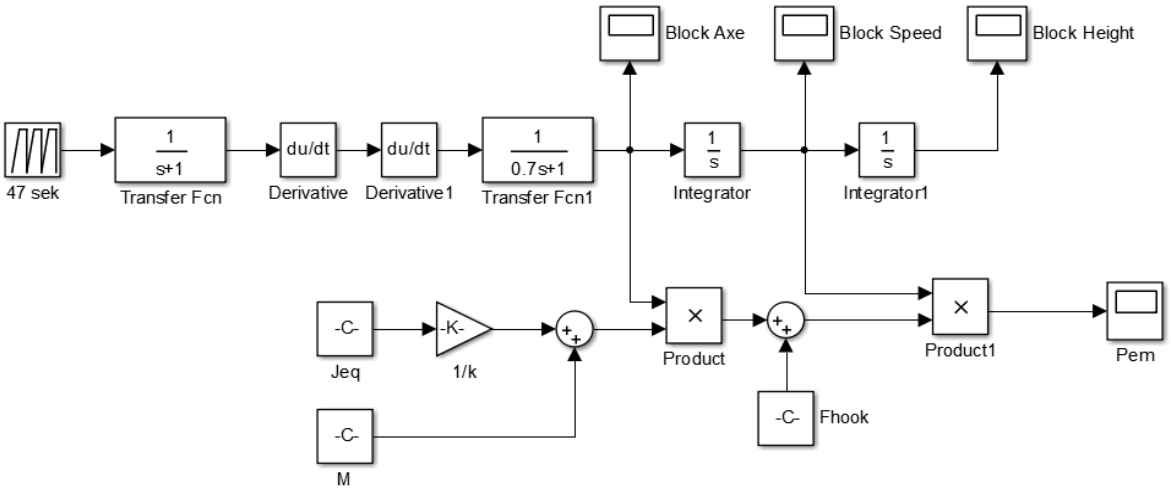

Figure A 4 - Model for generating power curves

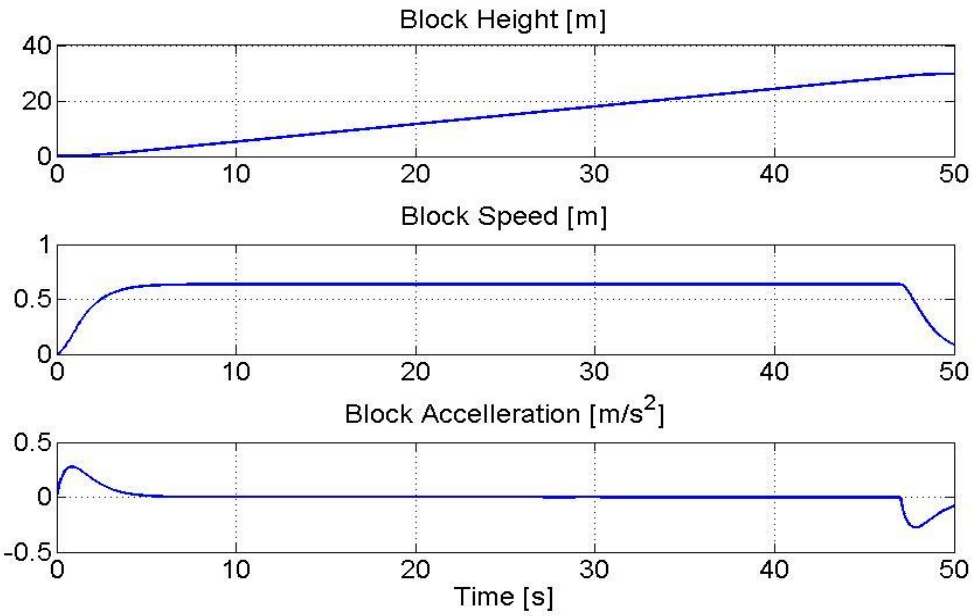

Figure A 5- Traveling block height, speed and acceleration

Appendix 6: Data for draw works motors

Model	GEB22A	GEB22D	GEB20B	GEB28A	GEB29A	GEB27A
Type	Horizontal	Horizontal	Vertical	Horizontal	Horizontal	Vertical
Application	Drawworks Mud Pump	Belt-Driven Mud Pump	Top Drive	Axial Load Drawworks	Side-Load Mud Pump	Top Drive
Available Certifications	ATEX, ABS	ATEX, ABS	ATEX, ABS	ATEX, ABS	ATEX, ABS	ATEX, ABS
Max. Continuous HP	1150	1150	1150	1500	1500	1500
Full Load RPM	800-1800	800-1800	800-1800	900-1200	900-1200	900-1200
Maximum RPM	3000	3000	2300	3000	3000	2300
Full Load Current	1120	1120	1120	1360	1360	1360
Torque (at base rpm)	7550	7550	7550	8750	8750	8750
Voltage	600-690 vac	600-690 vac	600-690 vac	600-690 vac	600-690 vac	600-690 vac
Inertia ($ftlb^2$)	429	429	429	767	767	767
Approximate Weight (lbs)	6500	6500	6000	8500	8500	7878

Figure A 6 - GEB motor data